A Lifshitz–Slyozov type model for adipocyte size dynamics: limit from Becker–Döring system and numerical simulation

Léo Meyer, Magali Ribot, Romain Yvinec

A Lifschitz-Slyozov type model for adipocyte size dynamics : limit from Becker-Döring system and numerical simulation

Léo Meyer, Magali Ribot, Romain Yvinec

A Lifschitz-Slyozov type model for adipocyte size dynamics : limit from Becker-Döring system and numerical simulation

Léo Meyer* *[1], Magali Ribot[1], and Romain Yvinec[2,3]

[1]Université d'Orléans, Institut Denis Poisson, Orléans, France
[2]Université Paris-Saclay, Inria, Centre Inria de Saclay, Palaiseau, France
[3]RC, INRAE, CNRS, Université de Tours, Nouzilly, France

March 6, 2023

Abstract

Biological data show that the size distribution of adipose cells follows a bimodal distribution. In this work, we introduce a Lifshitz-Slyozov type model, based on a transport partial differential equation, for the dynamics of the size distribution of adipose cells. We prove a new convergence result from the related Becker-Döring model, a system composed of several ordinary differential equations, toward mild solutions of the Lifshitz-Slyozov model using distribution tail techniques. Then, this result allows us to propose a new advective-diffusive model, the second-order diffusive Lifshitz-Slyozov model, which is expected to better fit the experimental data. Numerical simulations of the solutions to the diffusive Lifshitz-Slyozov model are performed using a well-balanced scheme and compared to solutions to the transport model. Those simulations show that both bimodal and unimodal profiles can be reached asymptotically depending on several parameters. We put in evidence that the asymptotic profile for the second-order system does not depend on initial conditions, unlike for the transport Lifshitz-Slyozov model.

1 Introduction

White adipose tissue is mainly composed of cells, called adipocytes, which store lipids in the body under the form of triglyceride droplets. Experiments in most animals [20, 19, 37] show that the size distribution of adipocytes follows a striking bimodal distribution with a large peak for small adipocytes around the minimal radius, see Fig. 1. The changes in volume of an adipocyte are governed by two opposite phenomena : lipogenesis, that is to say size increase by triglyceride intake, and lipolysis, that is to say size decrease through the hydrolyze of triglycerides and the excretion of fatty acids. Modeling the dynamics of size evolution of adipocytes is of great interest in order to study metabolic disorders, such as obesity or type 2 diabetes. Correlation between such diseases and the size and metabolism of adipose cells has been well established in the biological literature. Indeed, in [38], authors show that the size of an adipose cell has a strong correlation with its insulin sensitivity. As such, large cells are less sensitive, therefore a higher body weight leads to greater risks of type 2 diabetes. This study also shows that adipose tissue are very heterogeneous in terms

*leo.meyer@univ-orleans.fr

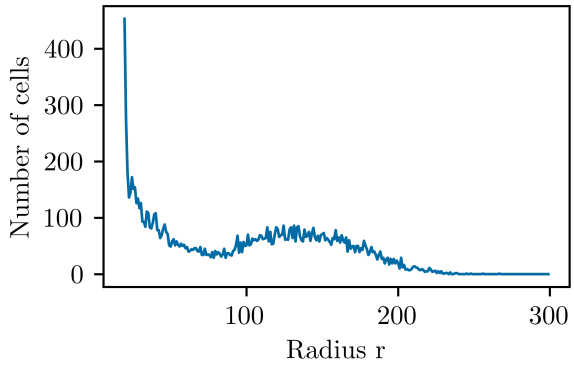

Figure 1: Example of the distribution of adipocytes in a rat biopsy. Credits : H. Soula

of size of cells. Those findings have also been described in [26], where the authors show that the adipose tissue is composed of cells that are different both molecularly and phenotypically.

Some computational models have also been used to provide insights into the adipose tissue physiology. In [22], the authors use an ODE model to investigate the role of lipases in the biochemistry of lipids. They are able to show that determining the active metabolic subdomain in the tissue is the key for accurate simulations, as well as the different activation rates of lipases for diglyceride and triglyceride breakdown. The rate of lipid turnover has also been studied in [1], where a decrease of the lipid release rate is correlated with the age of the individual. Finally, there are strong links between the adipose tissue and its extracellular matrix, and in case of obesity, one may observe tissue fibrosis such as described in [11]. In [30, 31], adipose tissue is modeled by a 2D agent-based model which takes into account the mechanical interactions between adipose cells and fibers forming the extra-cellular matrix. The authors study the spatial distribution of adipocytes under the form of lobules or in the case of tissue regeneration.

However, only a few mathematical models have been proposed in order to describe the size dynamics of adipose cells and no previous work has tackled a mechanistic understanding of the bimodal feature of adipocyte size distribution.

A first model has been derived by Jo, Periwal et al. in [21, 19] using a PDE for the adipose cell growth with a phenomenological cell growth rate. They are able to recover the bimodal feature of distributions as well as to perform some curve fitting on biological data. In [37] and later in [36], the authors describe the velocity of size change of adipocytes by biological considerations for lipogenesis and lipolysis, leading thus to some transport PDE models. They obtain bimodal distributions by using stochastic variations of the parameters. In [13], the authors perform the analysis and numerical simulations for a size-structured model describing the evolution of a set of adipocytes, including the creation of new adipocytes through differentiation processes from mesenchymal cells and preadipocytes, and accounting for a size velocity inversely proportional to the total surface of adipocytes. Finally, in [32], authors use an ODE model to investigate interplay and feedback loop between inflammatory response of bigger adipose cells and the immune system, which may lead to type 2 diabetes. The size of adipocytes is updated at each time step according to some probability of swelling and by a factor depending on the surplus of calories intake. However they do not concern themselves with the size distribution but with the whole tissue inflammation and the body wheight dynamic.

1.1 Transport equation for adipocyte size evolution

Following the work in [37], we first describe intake and release of lipids trough the cellular membrane, thus describing how the size of an adipose cell evolves. This will in turn allow us to build a model based on continuity equations.

Our first assumption will be the correlation between the amount of storage in an adipose cell and its radius. Cells shall be considered as spheres of a certain radius r, and the amount of lipids in the cell is denoted by x. Let us denote by $r(x)$ the radius of a cell containing x amount of lipids, by V_0 the volume of an empty cell and by V_{lipids} the molar volume of triglycerides.

We express the total volume of the cell in two different ways and we obtain the following relation:

$$V_{\text{lipids}}x + V_0 = \frac{4}{3}\pi r(x)^3,$$

which leads to :

$$r(x) = \left(\frac{3}{4\pi}(V_{\text{lipids}}x + V_0)\right)^{\frac{1}{3}}. \tag{1}$$

We also denote by L the amount of external lipids in the medium.

Henceforth, x will be considered as the size of our cell. Its variation $\frac{\mathrm{d}x}{\mathrm{d}t}$ depends on two flows : the intake of lipids by the cell from the medium and the release of lipids in the medium. As those two flows go through the membrane of the cell, they should be surface limited. We will also consider fast diffusion of the lipids in the medium so that the amount of lipids available for each cell is the same.

The intake term is a product of three factors :

- a term for a surface limited flow $\alpha r(x)^2$, where the constant α is the rate of this flow ;
- a Hill-like term with a radius cutoff ρ to describe resistance toward indefinite intake of lipids $\dfrac{\rho^n}{r(x)^n + \rho^n}$;
- a term that accounts for the available amount of lipids in the medium, in the form of a Michaelis-Menten term $\dfrac{L}{L+\kappa}$ with a saturation effect when the amount of external lipids L is large, with κ giving the order of magnitude of the threshold.

The release is a product of two terms :

- a term with a basal level of release β and a surface limited flow $\gamma r(x)^2$, where the constant γ is the release equivalent of the constant α ;
- a Michaelis-Menten term for the available amount of lipids in the cell $\dfrac{x}{x+\chi}$, where χ is the equivalent of κ for the release.

The variation $\dfrac{\mathrm{d}x}{\mathrm{d}t}$ can therefore be expressed as the difference between intake and release as :

$$\frac{\mathrm{d}x}{\mathrm{d}t} = \underbrace{\alpha r(x)^2 \frac{\rho^n}{r(x)^n + \rho^n}\frac{L}{L+\kappa}}_{\text{intake}} - \underbrace{(\beta + \gamma r(x)^2)\frac{x}{x+\chi}}_{\text{release}}. \tag{2}$$

We can now build a transport equation for the distribution $f(t,x)$ of adipose cells by amount of lipids $x \geq 0$ at time t. According to Eq. (2), the transport velocity will be given by :

$$v(x,L) = a(x)\frac{L}{L+\kappa} - b(x), \tag{3}$$

where

$$a(x) = \alpha r(x)^2 \frac{\rho^n}{r(x)^n + \rho^n} \tag{4}$$

and

$$b(x) = (\beta + \gamma r(x)^2)\frac{x}{x+\chi}. \tag{5}$$

Consequently, the function f satisfies the following transport equation :

$$\partial_t f(t,x) + \partial_x(v(x,L)f(t,x)) = 0, \qquad x \geq 0, \qquad t > 0. \tag{6}$$

We now need to describe the behaviour of the available amount of lipids in the medium L. As per our assumption, the total quantity of lipids in our system, denoted by λ, should be constant. There are two types of lipids in the system : the ones contained in the cells, and the lipids in the medium and we therefore have the following equality :

$$L(t) + \int_{\mathbb{R}_+} x f(t,x)\mathrm{d}x = \lambda. \tag{7}$$

Another hypothesis is that the number of adipocytes does not change in time. Thus, in regards to boundary conditions, we want to preserve the total population number and therefore we impose that :

$$\int_{\mathbb{R}_+} f(t,x)\mathrm{d}x = \int_{\mathbb{R}_+} f^0(x)\mathrm{d}x = m \text{ for all } t > 0. \tag{8}$$

This leads for Eq. (6) to boundary condition

$$(v(x,L(t))f(t,x))\big|_{x=0} = 0\,, \quad \text{for all } t > 0\,. \tag{9}$$

Notice that by Eqs. (4)-(5), we have $b(0) = 0$ and $a(0) > 0$. Hence, the boundary conditions (9) is equivalent to the Dirichlet boundary condition :

$$f(t,x)\big|_{x=0} = 0 \text{ for all } t > 0. \tag{10}$$

To sum up, the transport model for adipose cells with initial conditions (f^0, L^0), that will be called first-order Lifshitz-Slyozov model in the following, reads as:

$$\begin{cases} \partial_t f(t,x) + \partial_x(v(x,L(t))f(t,x)) = 0, & \text{(11a)} \\ L(t) + \displaystyle\int_{\mathbb{R}_+} x f(t,x)\mathrm{d}x = \lambda, & \text{(11b)} \\ (v(x,L(t))f(t,x))\big|_{x=0} = 0, & \text{(11c)} \\ f(0,x) = f^0(x) \text{ and } L(0) = L^0. & \text{(11d)} \end{cases}$$

1.2 New models for adipose tissue dynamics

In this subsection, we present the various models under consideration in this article. Starting from the description of lipogenesis and lipolysis as done in Eq. (4) and (5) following [37], we build size-structured PDE model following the framework of Becker-Döring system [4] and Lifshitz-Slyozov equations [27] initially derived for polymerization.

The aim of this model is to reproduce the adipocyte size distributions observed experimentally and their bimodal structure. However, the transport equation (6) possesses asymptotic solutions as a linear combination of Dirac masses centered on the zeros of the asymptotic speed. To recover the bimodality, we are therefore lead to introduce a diffusion term in the equation : we can either add a diffusion term with a constant rate with no real biological meaning, or we can compute a time and space dependent diffusion term coming from the discrete nature behind the Lifshitz-Slyozov formalism [16, 39]. For that purpose, we come back to a Becker-Döring system of ODEs giving the evolution with respect to time of the number of adipocytes with discrete sizes and from this, we derive a second order Lifshitz-Slyozov equation with a diffusion term.

Therefore, in the following, we will consider three different models for the size distribution of an adipocyte population, namely

- the ODE system (13) with discrete sizes, a variant of the Becker-Döring model.
- the previously published transport equation (11), also called first order Lifshitz-Slyozov equation,
- the transport-diffusion equation (17), the second order Lifshitz-Slyozov equation.

In all three models, the lipogenesis and lipolysis rate will be given by Eq. (4) and (5), respectively.

Note that we impose in all three models two conservation laws: (i) the conservation of the total amount of lipids and (ii) the conservation of the total number of adipocytes. Therefore, all these models have a constant population number and are coupled with a lipid conservation equation which ensures that the sum of the lipids in the external medium and the lipids inside the cells is constant.

1.2.1 A brief insight in Becker-Döring and Lifshitz-Slyozov equations

Becker-Döring equations have been introduced in [4] to model polymers undergoing aggregation and fragmentation. The Lifshitz-Slyozov model was introduced in [27] and first used for nucleation in super-saturated solid solutions and polymerisation processes. A rigourous treatment of the mathematical properties of the Becker-Döring equations was given by [3]. The relation between Becker-Döring equations and Lifshitz-Slyozov model goes back to [29]. For a detailed review of both models, see [17] and references therein.

Let us explain briefly the idea of these models for polymers. We denote by c_i, the amount of polymers containing i monomers for $i \in \mathbb{N}^*$ and hence c_1 stands for the amount of monomers. A polymer of size i denoted p_i can gain one monomer and grow to p_{i+1} with rate a_i or lose one monomer and shrink to p_{i-1} with rate b_i. We may write as a system of ODEs for the time evolution of the number of polymers c_i, one for each size i. Furthermore, the total amount of monomers, i.e free monomers and monomers within polymers, is assumed constant, which leads to a conservation equation. Stationary solutions of the Becker-Döring equations can be easily computed, and long time behavior has been characterized by [3].

Another possibility for the modeling of polymerisation-fragmentation processes is to describe continuously the size of polymers through a variable $x \in \mathbb{R}$. The distribution of polymers of size x at time t is therefore denoted by $f(t, x)$ and the quantity of monomers at time t is denoted by $L(t)$.

The distribution is classically transported as in Eq.(6) with speed $v(x, L) = a(x)L(t) - b(x)$ where $a(x)$ is the rate of polymerisation for size x and $b(x)$ is the rate of depolymerisation for size x. As previously, the total amount of monomers is conserved. Depending on the sign of $a(0)L(t) - b(0)$, boundary conditions should be provided for the system, see [10] for example.

After an adapted rescaling, it has been shown in various papers [9, 10, 24, 28, 34, 39] that the solutions to Becker-Döring system tend to the solutions to Lifshitz-Slyozov model. Formally, the limit up to second order can be considered and gives rise to an advection-diffusion equation as computed in [16, 39]. Existence of solutions is widely known for both models, see the seminal paper [3] for the Becker-Döring model and [6, 8] for the Lifshitz-Slyozov model..

Remark that Becker-Döring and Lifshitz-Slyozov equations have already been used in various contexts, for example modeling of biological phenomena, such as prions [12, 25, 35], [33], [15] or modeling in oceanography, see [40, 18].

1.2.2 A Becker-Döring model for adipose cells

Now, let us explain how we adapt this formalism to derive new models for adipocyte size dynamics. The purpose of this construction is to investigate the classical convergence theorems from Becker-Döring to Lifshitz-Slyozov and deduce the form of a diffusion term to add in our model.

We mention the main differences with the classical Becker-Döring and Lifshitz-Slyozov systems for polymerisation. First, velocity (2), arising from biological considerations, possesses three zeros for a well-chosen range of parameters which leads to bimodal asymptotic distributions, whereas classical choices for a and b are constant or power laws of x, which yields the existence of a single positive root. See also [5] for a polymerisation-fragmentation model without diffusion giving rise to bimodal asymptotics. Second, in our model, external lipids L cannot be assimilated to monomers c_1 and the conservation law (7) is therefore not the same as in the usual polymerisation models. Moreover, the saturation term $\dfrac{L}{L+\kappa}$ is not common in polymerisation modeling. Finally, our model conserves the total population number due to the boundary condition (11c), which adds an additional conservation law compared to the classical Becker-Döring model.

We shall now consider that an adipose cell is a bundle of smaller vesicles of typical size Λ. Hence the size of a cell can be defined by the number of vesicles it contains. We denote by c_i the number of cells of size i and by l the number of vesicles in the medium. A cell will aggregate a new vesicle with speed $a_i M(l)$,where $M(l) = \frac{l\Lambda}{l\Lambda+\kappa}$ following Eq. (2), and loose a vesicle at speed b_i, following this reaction :

$$\Lambda + i\Lambda \underset{b_{i+1}}{\overset{a_i M(l)}{\rightleftharpoons}} (i+1)\Lambda.$$

Following a rescaling procedure, which is described in details in Annex 7, we define $c^\varepsilon = (c_i^\varepsilon)_{i\geq 0}$ and $J_i^\varepsilon(c^\varepsilon, L^\varepsilon)$ the flow of the previous reaction given by :

$$J_i^\varepsilon(c^\varepsilon, L^\varepsilon) = a_i^\varepsilon \frac{L^\varepsilon}{L^\varepsilon + \kappa} c_i^\varepsilon - b_{i+1}^\varepsilon c_{i+1}^\varepsilon,\ i \geq 0, \tag{12}$$

where a_i^ε (resp. b_i^ε) are discrete counterpart of the continous function a defined at Eq.(4) (resp. b defined at Eq.(5)), see Sec.2 for more details.

Similarly as before, see Eq. (7), L^ε will satisfy an equation accounting for conservation of the amount of lipids and we get the following ODE system :

$$\begin{cases} \dfrac{dc_i^\varepsilon}{\mathrm{d}t} = \dfrac{1}{\varepsilon}(J_{i-1}^\varepsilon(c^\varepsilon, L^\varepsilon) - J_i^\varepsilon(c^\varepsilon, L^\varepsilon)),\ \forall i \geq 1, & \text{(13a)} \\ \dfrac{dc_0^\varepsilon}{\mathrm{d}t} = -\dfrac{1}{\varepsilon} J_0^\varepsilon(c^\varepsilon, L^\varepsilon), & \text{(13b)} \\ L^\varepsilon(t) + \displaystyle\sum_{i=0}^{\infty} i\varepsilon^2 c_i^\varepsilon(t) = \lambda,\ \forall t \geq 0, & \text{(13c)} \\ L^\varepsilon(0) = L^{\varepsilon,0}, \quad c_i^\varepsilon(0) = c_i^{\varepsilon,0},\ \forall i \geq 1, & \text{(13d)} \end{cases}$$

which is similar to Becker-Döring equations except for the definition of the flux J_i^ε (saturing fluxes of monomers), and the minimal size is 0 and not 1. Observe also that there is no 'boundary' flux, thus the quantity

$$m = \varepsilon \sum_{i \geq 0} c_i^\varepsilon(t) \text{ is constant in time.} \tag{14}$$

This is the discrete analogous to the previous conservation (8) of the zeroth order moment of f.

A solution to the previous system exists according to Theorem 2.1 recalled in Sec.2. Now let us define the following step functions depending on both time and space :

$$f^\varepsilon(t,x) = \sum_{i \geq 0} \mathbb{1}_{\Gamma_i^\varepsilon}(x) c_i^\varepsilon(t),$$

where $\Gamma_i^\varepsilon = [(i - \frac{1}{2})\varepsilon, (i + \frac{1}{2})\varepsilon[$, and $(c_i^\varepsilon)_{i \geq 0}$ is a solution to (13).

Convergence of function f^ε when $\varepsilon \to 0$ towards a solution f of the Lifshitz-Slyozov equation (11) is a classical result, see Theorem 2.3 recalled in Sec.2. In the present work, we prove that a similar convergence result hold in a stronger topology, and with a control of the speed of convergence, of order at least ε.

To that, we introduce the tail distributions :

$$F(t,x) = \int_x^\infty f(t,y)\mathrm{d}y, \qquad F^\varepsilon(t,x) = \int_x^\infty f^\varepsilon(t,y)\mathrm{d}y.$$

The main analytical result of this article is the following theorem, whose more rigorous statement will be specified later in Theorem 3.1:

Theorem (Convergence of tails of distributions)**.** *Under some hypotheses detailed in Sec.2 and 3, there exists some constant $K > 0$ and some time $T > 0$ such that for all $t \in (0,T)$ and for ε small enough :*

$$|L^\varepsilon(t) - L(t)| + \int_{\mathbb{R}_+} |F^\varepsilon(t,x) - F(t,x)|\mathrm{d}x \leq \varepsilon K\,.$$

This result provides a new approach for looking into convergence from Becker-Döring to Lifshitz-Slyozov. Contrary to more classical results where convergence towards a weak solution is achieved using Ascoli-Arzela's Theorem, this theorem yields convergence towards mild solutions and gives a bound of order ε on the speed of this convergence.

1.2.3 A second order Lifshitz-Slyozov model

Another goal in this article is to derive a new model with a diffusive term from Becker-Döring system (13). One can see this diffusive term as a second order term emerging from the convergence theorem

3.1. There are various ways to yield this term, see for example [39], [34], [10]. The derivation of the diffusive term will be detailed in Section 4, but we present the model here for the sake of completeness.

The so-called second order Lifshitz-Slyozov model therefore takes the form of a transport-diffusion equation, with a diffusive term which depends both on x and $L(t)$, i.e. :

$$\partial_t g + \partial_x(vg) = \frac{\varepsilon}{2}\partial_x^2(dg), \qquad \forall x \geq 0,$$

where

$$d : (x, L) \in \mathbb{R}_+ \times \mathbb{R}_+ \to d(x, L) = a(x)\frac{L}{L+\kappa} + b(x). \tag{15}$$

We need to complement this PDE with adapted boundary conditions. Since we want the conservation of the zeroth order moment denoted by $\int_{\mathbb{R}_+} g(t,x)\mathrm{d}x = m$, we need to impose the following null-flux boundary condition :

$$(-vg + \frac{\varepsilon}{2}\partial_x(dg))\Big|_{x=0} = 0. \tag{16}$$

Therefore, we consider the following system, which consists of the previous PDE and boundary conditions, complemented by previous constraint (7) and initial conditions for g and L :

$$\begin{cases} \partial_t g + \partial_x(vg) = \frac{\varepsilon}{2}\partial_x^2(dg), & \text{(17a)} \\ L(t) + \int_{\mathbb{R}_+} xg(t,x)\mathrm{d}x = \lambda, & \text{(17b)} \\ \Big(- vg + \frac{\varepsilon}{2}\partial_x(dg)\Big)\Big|_{x=0} = 0, & \text{(17c)} \\ g(0,x) = g^0(x) \text{ and } L(0) = L^0. & \text{(17d)} \end{cases}$$

We provide interesting numerical evidence of stationary solutions of the advection-diffusion model (17) following a bimodal distribution. The numerical simulations are performed using a well-balanced scheme developped in [14]. We also demonstrate that to observe a bimodal asymptotics, parameters should be taken into an adapted parameter range.

1.3 Outline of the article

In Section 2, we will give some preliminary results on the existence of solutions to systems (13) and (11). In Section 3, we will show the convergence theorem thanks to the tail of distributions technique. Then, in Section 4, we derive formally the second-order Lifshitz-Slyozov model, that is to say system (17) and we give the expression for its stationary solutions. In Section 5, we display some numerical results and we show that bimodality of the stationary solution can be observed in well-chosen parameter range. Finally, we discuss our results in Section 6. We also recall the rescaling procedure of (13) in annex 7.

2 Preliminary results

In this section, we give the main already-known results of existence of solutions to systems (13) and (11) and convergence of solutions to system (13) towards (11). Proofs have been easily adapted to our framework.

2.1 Existence results on Becker - Döring system

We consider first the Becker - Döring system (13) for fixed ε.

We assume that there exist some strictly positive constants A, B, C_a, C_b, K_a, K_b and δ such that for all $i \geq 0$:

$$a_i^\varepsilon \leq C_a \text{ and } b_i^\varepsilon \leq C_b i\varepsilon, \tag{H'1}$$

$$|a_i^\varepsilon - a_{i+1}^\varepsilon| \leq K_a\varepsilon \text{ and } |b_i^\varepsilon - b_{i+1}^\varepsilon| \leq K_b\varepsilon. \tag{H'2}$$

We define the state space for Eq. (13) by

$$X := \{x = (x_i)_{i\geq 0} \in \mathbb{R}_+^{\mathbb{N}} : \sum_{i=0}^{+\infty} i x_i < \infty\},$$

endorsed with the norm $\|x\|_X = \sum_{i=0}^{+\infty} i|x_i|$. We denote $x \geq 0$ if $x_i \geq 0$ for all $i \geq 0$, and $X^+ := \{x \in X : x \geq 0\}$. We give the following definition of solution to Eq. (13):

Definition 2.1. *Let $T > 0$ and $\varepsilon > 0$. A solution $(c^\varepsilon, L^\varepsilon)$ of (13) in $[0,T)$ is a couple of a function $L^\varepsilon : [0,T) \to \mathbb{R}$ and a sequence of functions $c^\varepsilon = (c_i^\varepsilon)_{i\geq 0}$, $c_i^\varepsilon : [0,T) \to X$ such that :*

(i) For all $t \in [0,T)$, $L^\varepsilon(t) \geq 0$ and $c^\varepsilon(t) \in X^+$,

(ii) For all $i \geq 1$, $c_i^\varepsilon : [0,T) \to \mathbb{R}$ is continuous and $\sup_{t\in[0,T)} \|c^\varepsilon(t)\|_X < +\infty$,

(iii) $L^\varepsilon : [0,T) \to \mathbb{R}$ is continuous and $\sup_{t\in[0,T[} |L^\varepsilon(t)| < +\infty$,

(iv) For all $t \in [0,T)$, $\int_0^t \sum_{i=0}^{+\infty} a_i^\varepsilon c_i^\varepsilon(s)\mathrm{d}s < \infty$ and $\int_0^t \sum_{i=0}^{+\infty} b_i^\varepsilon c_i^\varepsilon(s)\mathrm{d}s < \infty$,

(v) For all $t \in [0,T)$, for all $i \geq 1$:

$$c_i^\varepsilon(t) = c_i^{\varepsilon,0} + \frac{1}{\varepsilon}\int_0^t [J_{i-1}^\varepsilon(c^\varepsilon(s), L^\varepsilon(s)) - J_i^\varepsilon(c^\varepsilon(s), L^\varepsilon(s))]\mathrm{d}s,$$

$$c_0^\varepsilon(t) = c_0^{\varepsilon,0} - \frac{1}{\varepsilon}\int_0^t J_0^\varepsilon(c^\varepsilon(s), L^\varepsilon(s))\mathrm{d}s,$$

$$L^\varepsilon(t) = L^{\varepsilon,0} - \varepsilon\int_0^t \sum_{i=0}^{+\infty} J_i^\varepsilon(c^\varepsilon(s), L^\varepsilon(s))\mathrm{d}s$$

Well-posedness of solutions to (13) as defined at Def.2.1 can be shown by finite dimensional approximation, using the method developped in [3] :

Theorem 2.1. *Let $T > 0$ and $\varepsilon > 0$. Let $L^{\varepsilon,0} \in \mathbb{R}_+$ et $c^{\varepsilon,0} \in X^+$ such that $L^{\varepsilon,0} + \sum_{i=0}^{+\infty} i\varepsilon^2 c_i^{\varepsilon,0} = \lambda < \infty$. Assume that* (H'1), (H'2) *hold true. Then there exists a unique solution $(c^\varepsilon, L^\varepsilon)$ to Becker - Döring system* (13) *in the sense of Def.2.1 which satisfies initial conditions $c^\varepsilon(0) = c^{\varepsilon,0}$ and $L^\varepsilon(0) = L^{\varepsilon,0}$.*

The uniqueness and conservation properties of the solution are obtained using the following proposition that will be needed later on, see Sec.4. In particular, the following proposition states that any solution of the Becker - Döring system (13) preserves the first two moments for all times, and provides the starting point to compute any admissible moments for the solution of the Becker - Döring system. In [3], we can find the following Theorem 2.5 that we reproduce here for the reader's convenience :

Proposition 2.1. *Let $(\phi_i)_{i\geq 0}$ be a given sequence. Let $(c^\varepsilon, L^\varepsilon)$ be the solution of (13) on $[0,T)$, $0 < T \leq +\infty$.*

Assume that for all $0 \leq t_1 < t_2 < T$, $\displaystyle\int_{t_1}^{t_2} \sum_{i=0}^{\infty} |\phi_{i+1} - \phi_i| a_i^\varepsilon c_i^\varepsilon(t)\mathrm{d}t < \infty$ and that either of the following holds :

(a) $\phi_i = \mathcal{O}(i)$ and $\displaystyle\int_{t_1}^{t_2} \sum_{i=0}^{\infty} |\phi_{i+1} - \phi_i| b_{i+1}^\varepsilon c_{i+1}^\varepsilon(t)\mathrm{d}t < \infty$ or

(b) $\displaystyle\sum_{i=0}^{\infty} \phi_i c_i^\varepsilon(t_k) < \infty$, for $k = 1, 2$ and $\phi_{i+1} \geq \phi_i \geq 0$ for i large enough.

Then :

$$\sum_{i=0}^{\infty} \phi_i c_i^\varepsilon(t_2) - \sum_{i=0}^{\infty} \phi_i c_i^\varepsilon(t_1) + \int_{t_1}^{t_2} \sum_{i=0}^{\infty} \frac{\phi_{i+1} - \phi_i}{\varepsilon} b_{i+1}^\varepsilon c_{i+1}^\varepsilon(t)\mathrm{d}t = \int_{t_1}^{t_2} \sum_{i=0}^{\infty} \frac{\phi_{i+1} - \phi_i}{\varepsilon} a_i^\varepsilon \frac{L^\varepsilon(t)}{L^\varepsilon(t) + \kappa} c_i^\varepsilon(t)\mathrm{d}t.$$

2.2 Lifschitz-Slyozov system and classical convergence result

Even though we have precise forms for the intake and release functions, for the sake of generality we make the following assumptions on functions a and b occurring in Eq. (3) :

$$a, b \in C^1(\mathbb{R}_+, \mathbb{R}_+), \tag{H1}$$

$$a(0) > 0 \text{ and } \sup_{x\in\mathbb{R}_+} |a(x)| = C_a, \tag{H2a}$$

$$|b(x)| \leq C_b x \text{ for all } x \in \mathbb{R}_+ \text{ and } \lim_{R\to\infty} \sup_{x\geq R} \frac{b(x)}{x} = 0, \tag{H2b}$$

$$\sup_{x\in\mathbb{R}_+} |a'(x)| = K_a \text{ and } \sup_{x\in\mathbb{R}_+} |b'(x)| = K_b, \tag{H3}$$

with $C_a, C_b, K_a, K_b > 0$. We first define measured-valued solutions to the Lifschitz-Slyozov system (11), following [8]

Definition 2.2. *Given an initial condition $(f^0, L^0) \in C^0(\mathbb{R}_+) \cap L^1(\mathbb{R}_+, (1+x)\mathrm{d}x) \times \mathbb{R}_+$, a measured-valued solution to system (11) is composed of two functions $f \in C(0,T; \mathcal{M}^1(0,\infty) - weak - *)$ and $L \in C(0,T)$ such that for all $0 < t < T$ and for all $\varphi \in C^1([0,T] \times \mathbb{R}_+)$ the following relations hold:*

$$\int_0^T \int_{\mathbb{R}_+} (\partial_t \varphi(t,x) + v(x, L(t)) \partial_x \varphi(t,x)) f(t, \mathrm{d}x) + \int_{\mathbb{R}_+} \varphi(0,x) f^0(x)\mathrm{d}x = 0,$$

$$L(t) + \int_{\mathbb{R}_+} x f(t, \mathrm{d}x) = \lambda.$$

Now, let us state the convergence of solutions to Becker-Döring system towards solutions to Lifschitz-Slyozov system. In order to compare solutions to Becker-Döring system to solutions to Lifschitz-Slyozov system, we need to define the following piecewise constant functions. Let $\Gamma_i^\varepsilon = [(i-\frac{1}{2})\varepsilon, (i+\frac{1}{2})\varepsilon)$ and c_i^ε be solutions to (13), then we define

$$\begin{cases} f^\varepsilon(t,x) = \sum_{i\geq 0} \mathbb{1}_{\Gamma_i^\varepsilon}(x) c_i^\varepsilon(t)\,, & \text{(18a)} \\ a^\varepsilon(x) = \sum_{i\geq 0} \mathbb{1}_{\Gamma_i^\varepsilon}(x) a_i^\varepsilon\,, & \text{(18b)} \\ b^\varepsilon(x) = \sum_{i\geq 1} \mathbb{1}_{\Gamma_i^\varepsilon}(x) b_i^\varepsilon\,, & \text{(18c)} \end{cases}$$

where we assume that :

$$a_i^\varepsilon = a(i\varepsilon) \text{ and } b_i^\varepsilon = b(i\varepsilon), \text{ for all } i \geq 0 \text{ and } \varepsilon > 0. \tag{H4}$$

Given our definitions in Eq. (18), from Proposition 2.1 and with $\phi_i = \int_{\Gamma_i^\varepsilon} \phi(x)\mathrm{d}x$, we deduce the following proposition, that is the starting point to study the convergence of the solution of the Becker-Döring system (13) towards solution of the Lifshitz-Slyozov equation (11).

Proposition 2.2. *Let $\phi \in L^\infty(\mathbb{R}_+)$. Then for every $t \geq 0$, we have the following equality :*

$$\int_0^\infty \phi(x)(f^\varepsilon(t,x) - f^\varepsilon(0,x))\mathrm{d}x = \int_0^t \int_0^\infty (\Delta_\varepsilon \phi(x) a^\varepsilon(x) \frac{L^\varepsilon(t)}{L^\varepsilon(t)+\kappa} - \Delta_{-\varepsilon}\phi(x) b^\varepsilon(x)) f^\varepsilon(t,x)\mathrm{d}x\mathrm{d}t,$$

where

$$\Delta_\varepsilon \phi(x) = \frac{\phi(x+\varepsilon) - \phi(x)}{\varepsilon}. \tag{19}$$

Finally, we obtain the following convergence theorem from the Becker-Döring equations to the Lifshitz-Slyozov equations, as in [39]:

Theorem 2.2. *Consider an initial condition $(L^{\varepsilon,0}, (c_i^{\varepsilon,0})_{i\geq 0})$ and the corresponding solution $(L^\varepsilon, (c_i^\varepsilon)_{i\geq 0})$ in the sense of Definition 2.1. We assume that there exists a constant $K > 0$ and $0 < s \leq 1$ such that :*

- $L^{\varepsilon,0} + \varepsilon^2 \sum_{i\geq 0} i c_i^{\varepsilon,0} = \lambda$,
- $\varepsilon \sum_{i\geq 0} c_i^{\varepsilon,0} < K$,
- $\varepsilon \sum_{i\geq 0} (i\varepsilon)^{1+s} c_i^{\varepsilon,0} < K$.

We also assume hypotheses H1 - H4 to hold. Then there exists a sequence ε_n and a solution (f, L) to (11) in the sense of Def. 2.2 such that :

$$\begin{cases} f^{\varepsilon_n} \to f\,, \;\; x f^{\varepsilon_n} \to xf \text{ in } C^0([0,+\infty[; \mathcal{M}^1(0,+\infty) - weak - *), \\ L^{\varepsilon_n} \to L \text{ uniformly in } C^0([0,T]). \end{cases}$$

Now, let us consider the existence of mild solutions to (11). For that purpose, we first define the characteristic curves.

Assume $L \in C^0(\mathbb{R}_+)$ to be given. The characteristic curves associated to (11) are solutions to :

$$\begin{cases} \partial_s X(s;t,x) = v(X(s;t,x), L(s)), \\ X(t;t,x) = x. \end{cases}$$

Since v is C^1 in both x and L, the characteristics are uniquely defined and form an ordered family. We denote $I_{t,x}$ their maximal time interval and by $X_c(t) = X(t;0,0)$ the characteristic curve that is equal to 0 at time 0. Then, a mild solution to system (11) is given by the following definition :

Definition 2.3. *Given a smooth initial condition f^0 and $L \in C^0(\mathbb{R}_+)$, a mild solution of*

$$\begin{cases} \partial_t f + \partial_x(v(x, L(t))f) = 0, \\ (v(x, L(t))f(t,x))\big|_{x=0} = 0, \\ f(0,x) = f^0(x), \end{cases}$$

is given by :

$$f(t,x) = f^0(X(0;t,x)) \exp\left(- \int_0^t \partial_x v(X(s;t,x), L(s)) ds \right) \mathbb{1}_{(X_c(t),\infty)}(x).$$

A couple (f, L) is said to be a solution of (11) iff f is a mild solution associated to L and $L : \mathbb{R}_+ \to \mathbb{R}_+$ solves $L(t) + \int_{\mathbb{R}_+} x f(t,x) \mathrm{d}x = \lambda$ for all $t \geq 0$.

Remark. *Since we impose null-flux boundary conditions on this system : $v(x, L(t))f(t,x)|_{x=0} = 0$, there is no term involving "incoming characteristics" $\mathbb{1}_{(0,X_c(t))}(x)$.*

We follow the proofs in [8] and [6] and we obtain in a straightforward way the expected existence and uniqueness result :

Theorem 2.3. *Given an initial condition $(f^0, L^0) \in C^0(\mathbb{R}_+) \cap L^1(\mathbb{R}_+, (1+x)\mathrm{d}x) \times \mathbb{R}_+$ and assuming hypotheses* (H1)-(H3)*, Lifschitz-Slyozov system* (11) *has a unique solution on the interval $[0,T]$ in the sense of Def.2.3.*

Note that the mild solution given by Theorem 2.3 is also a weak solution in the sense of Definition 2.2, see [6], and under hypotheses (H1)-(H3) both definitions coincide.

3 A new convergence result from Becker-Döring to Lifschitz-Slyozov equations

In this part of our work we introduce a different way to see the convergence from the Becker-Döring equations to the Lifschitz-Slyozov equations. Using tail distributions allows to reduce the non linearity of our system by pulling the speed of advection outside of the space derivative. Tail distributions were also found to be useful to obtain a quasi comparison principle in [7] and to obtain refined uniqueness properties in [23, 6]. The main idea is to use results on the tail of the distributions to show convergence. Finally, we note that out result uses the fact that a solution to system (11) exists while the previous result also shows existence of solution of (11), by showing a convergence to a measure valued function which turns out to be a solution of (11).

Let $(f^\varepsilon, L^\varepsilon)$ be the solution of the Becker-Döring ODE system (13) and Eq. (18), and let (f, L) the mild solution of Lifshitz-Slyozov equations (11). We recall the tail distribution definition,

$$F(t,x) = \int_x^\infty f(t,y)\mathrm{d}y, \qquad F^\varepsilon(t,x) = \int_x^\infty f^\varepsilon(t,y)\mathrm{d}y\,, \tag{20}$$

and introduce their difference

$$E(t,x) = F^\varepsilon(t,x) - F(t,x)\,. \tag{21}$$

We introduce the following additional hypotheses to use in our main theorem :

$$\sup_{x\in\mathbb{R}_+} |a''(x)| < \infty \text{ and } \sup_{x\in\mathbb{R}_+} |b''(x)| < \infty, \tag{H5}$$

$$\sum_{i\geq 0} |c_{i+1}^{\varepsilon,0} - c_i^{\varepsilon,0}| < +\infty, \tag{H6}$$

$$\varepsilon \sum_{i\geq 0} i|c_{i+1}^{\varepsilon,0} - c_i^{\varepsilon,0}| < +\infty. \tag{H7}$$

$$\text{There exists some constant } \bar{L} > 0, \text{ such that } \inf_{\varepsilon>0} L^{\varepsilon,0} \geq \bar{L}. \tag{H8}$$

$$\text{There exists some constant } K > 0 \text{ such that } \sup_{\varepsilon>0} c_0^{\varepsilon,0} < K. \tag{H9}$$

We now state our main theorem.

Theorem 3.1. *Let $T > 0$. Suppose that there exists some constant $C_{\text{init}} > 0$ such that for all $\varepsilon > 0$, $\int_{\mathbb{R}_+} |E(0,x)|\mathrm{d}x \leq \varepsilon C_{\text{init}}$. Also assume that hypotheses* (H1)-(H9) *hold true. Then there exists some constant $C(T) > 0$ such that for $\varepsilon > 0$ small enough and for all $t \in [0,T]$:*

$$|L^\varepsilon(t) - L(t)| + \int_{\mathbb{R}_+} |E(t,x)|\mathrm{d}x \leq \varepsilon C(T).$$

The proof proceeds as follows. Taking inspiration from [23, 6], we first note that owing to the total population number conservation, the lipid terms can be controlled by the tail, $|L^\varepsilon(t) - L(t)| \leq \int_{\mathbb{R}_+} |E(t,x)|\mathrm{d}x$. The control on the tail relies on a Grönwall's lemma argument. For that purpose, we derive the equation followed by $F^\varepsilon(t,x)$ (Lemma 3.5). We point out that the case $x < \varepsilon/2$ has to be treated separately due to remaining boundary terms. This allows us to give a first estimate on the integral $\int_{\mathbb{R}_+} |E(t,x)|\mathrm{d}x$. We then make use of the mild solution formulation to derive the partial differential equation followed by F and in turn the one followed by E (Lemma 3.6). The proof follows by bounding the terms in the estimate on $\int_{\mathbb{R}_+} |E(t,x)|\mathrm{d}x$, and in particular we show that $F^\varepsilon(t,x)$ satisfies the same equation as F up to an order ε (Lemma 3.7). To this end, the key argument relies on refined estimates of the difference between the first order derivative of $F^\varepsilon(t,x)$ and its discrete analog. This estimate needs uniform control on the solutions c_i^ε of the Becker-Döring system and their increments $c_{i+1}^\varepsilon - c_i^\varepsilon$ (Subsection 3.1, Lemmas 3.1 to 3.4), which is new, up to our knowledge.

Hypotheses (H1) - (H4) are classical in the study of our model. However, other assumptions are less common but arise naturally from the result. Contrary to the classical convergence result, we work with mild solutions of the Lifshitz-Slyozov system. Hence, we need proper bounds on second

order terms. We shall see in Section 4 that those terms lead us to the second order Lifshitz-Syozov model. Nonetheless, those terms involve second order derivatives of both a and b which leads us to hypothesis (H5). Hypotheses (H6) and (H7) simply tell us that the initial condition for the Becker-Döring system must have finite zeroth order moment and first moment increments. Lemma 3.4 shows that this property propagates in time. Additional assumptions have to be made to obtain our main theorem. The assumption (H8) on the initial condition $L^{\varepsilon,0}$ is necessary since it leads to strict positivity of L^ε in finite time, uniformly in ε. The assumption (H9) on the initial condition $c_0^{\varepsilon,0}$ is technical and ensures that the proper boundary condition (11c) is satisfied for all times. Finally the assumption on $\displaystyle\int_{\mathbb{R}_+} |E(0,x)|\mathrm{d}x$ is made to conclude after using Grönwall's lemma at the very end of the proof. This assumption relates both initial conditions $(c_i^{\varepsilon,0})_{i\geq 0}$ and f^0. A fair choice for the initial condition $(c_i^{\varepsilon,0})_{i\geq 0}$ is $c_i^{\varepsilon,0} = f^0(i\varepsilon)$ for all $i \geq 0$. Then the assumption is verified as long as $(f^0)' \in L^1(\mathbb{R}_+, x\mathrm{d}x)$.

In all this section, we assume that hypotheses (H1) - (H9) hold true.

3.1 Preliminary results on Becker-Döring system

We start with a lemma that allows to control the lipid term away from 0, in the lines of previous results from [6].

Lemma 3.1. *A solution $(L^\varepsilon, c^\varepsilon)$ of (13) with $\lambda > 0$ verifies that there exists $C > 0$ such that for all $t > 0$,*

$$\inf_{\varepsilon>0} L^\varepsilon(t) \geq \bar{L}\exp(-Ct). \tag{22}$$

Proof. For all $t > 0$, we have, using the three first equations of system (13) :

$$\begin{aligned}\frac{\mathrm{d}L^\varepsilon(t)}{\mathrm{d}t} = -\varepsilon\sum_{i\geq 0} J_i^\varepsilon(c^\varepsilon(t), L^\varepsilon(t)) &= -\varepsilon\sum_{i\geq 0}\left(a_i^\varepsilon \frac{L^\varepsilon(t)}{L^\varepsilon(t)+\kappa} c_i^\varepsilon(t) - b_{i+1}^\varepsilon c_{i+1}\varepsilon(t)\right)\\ &\geq -\frac{L^\varepsilon(t)}{L^\varepsilon(t)+\kappa}\varepsilon\sum_{i\geq 0} a_i^\varepsilon c_i^\varepsilon(t),\end{aligned}$$

and thus, because $\sup_{x\in\mathbb{R}_+}|a(x)| = C_a$, and $\frac{L^\varepsilon}{L^\varepsilon+\kappa} \leq \frac{1}{\kappa}L^\varepsilon$:

$$\frac{\mathrm{d}L^\varepsilon(t)}{\mathrm{d}t} \geq -\frac{C_a}{\kappa}L^\varepsilon\int_{-\varepsilon/2}^{+\infty} f^\varepsilon(t,x)\mathrm{d}x$$

and by conservation of the moment (14), $\displaystyle\int_{-\varepsilon/2}^{+\infty} f^\varepsilon(t,x)\mathrm{d}x = \varepsilon\sum_{i\geq 0} c_i^\varepsilon(t) = m$,

$$\frac{\mathrm{d}L^\varepsilon(t)}{\mathrm{d}t} \geq -\frac{C_a m}{\kappa}L^\varepsilon.$$

We conclude by Grönwall's lemma and using Hypothesis (H8). □

We next state a lemma adapted from [10] that allows to obtain pointwise estimates of the density f^ε near the boundary, through the uniform propagation of exponential moments. For $x \in \mathbb{R}_+$ and $t > 0$, let

$$H^\varepsilon(t,x) = \sum_{i\geq 0} c_i^\varepsilon(t)\,\mathrm{e}^{-ix}\ .$$

Lemma 3.2. *Let $x \in \mathbb{R}_+^*$. Then there exist some constants $\tilde{K} > 0$ and $\varepsilon^* > 0$ such that for all $0 < \varepsilon < \varepsilon^*$:*

$$H^\varepsilon(t,x) \leq H^\varepsilon(0,x) + \tilde{K} \text{ for all } t > 0,$$

and in particular :

$$\text{for all } i \geq 0, \sup_{0<\varepsilon<\varepsilon^*} \sup_{t\in[0,T]} c_i^\varepsilon(t) \leq \bar{c}_i < +\infty. \tag{23}$$

Proof. Using Lemma 3.1, and the assumption (H8) on $L^\varepsilon(0)$, we have that $\inf_{\varepsilon>0} \inf_{t\in(0,T]} L^\varepsilon(t) \geq \bar{L}\exp(-CT)$. Thus we can find a constant $c > 0$ such that :

$$\inf_{\varepsilon>0} \inf_{t\in(0,T]} \frac{L^\varepsilon(t)}{L^\varepsilon(t)+\kappa} \geq c.$$

Now we choose $\delta > 0$ such that $c > 2\delta$. Using Taylor's expansion, we have $a(i\varepsilon) = a(0) + i\varepsilon a'(0) + \mathcal{O}((i\varepsilon)^2)$. Then with hypotheses (H2b) and (H3) and for ε small enough, we find that $a(i\varepsilon) \geq \frac{3}{4}(a(0) - i\varepsilon K_a) > 0$. Therefore we have that for ε small enough :

$$\forall i \leq \frac{1}{\sqrt{\varepsilon}},\ a(i\varepsilon) \geq \frac{a(0)}{2}. \tag{24}$$

In turn, by hypotheses (H2a), (H2b) and (H4), we have that for ε small enough and for all $i \leq \frac{1}{\sqrt{\varepsilon}}$:

$$\frac{b_i^\varepsilon}{a_i^\varepsilon} = \frac{b(i\varepsilon)}{a(i\varepsilon)} \leq 2C_b \frac{\sqrt{\varepsilon}}{a(0)} \xrightarrow[\varepsilon\to 0]{} 0.$$

Let $x \in \mathbb{R}_+^*$. Hence, one can find $\varepsilon^* > 0$ such that :

$$\sup_{\varepsilon<\varepsilon^*} \sup_{i\leq\frac{1}{\sqrt{\varepsilon}}} |\frac{b_i^\varepsilon}{a_i^\varepsilon}| \leq \delta\, \mathrm{e}^{-x}.$$

This gives us that for ε^* small enough, $\varepsilon < \varepsilon^*$ and $i \leq \frac{1}{\sqrt{\varepsilon}}$:

$$\frac{L^\varepsilon(t)}{L^\varepsilon(t)+\kappa} - \frac{b_i^\varepsilon}{a_i^\varepsilon}\,\mathrm{e}^x \geq 2\delta - \delta = \delta. \tag{25}$$

Now we proceed with the bound on H^ε using Eq.(13) and (12) :

$$\begin{aligned}
\varepsilon\partial_t H^\varepsilon(t,x) &= (\mathrm{e}^{-x}-1)\sum_{i\geq 0} J_i^\varepsilon(c)\,\mathrm{e}^{-ix} \\
&= (\mathrm{e}^{-x}-1)\left[\frac{L^\varepsilon(t)}{L^\varepsilon(t)+\kappa} a_0^\varepsilon c_0^\varepsilon(t) + \sum_{i\geq 1} a_i^\varepsilon\Big(\frac{L^\varepsilon(t)}{L^\varepsilon(t)+\kappa} - \frac{b_i^\varepsilon}{a_i^\varepsilon}\,\mathrm{e}^x\Big) c_i^\varepsilon(t)\,\mathrm{e}^{-ix}\right].
\end{aligned}$$

Now we split the sum on the right depending on $\frac{1}{\sqrt{\varepsilon}}$ with ε small enough as before. Note that since $x > 0$, we have that $(\mathrm{e}^{-x}-1) < 0$. The first sum is treated using (25) and the bound (24) :

$$\varepsilon\partial_t H^\varepsilon(t,x) \le (\mathrm{e}^{-x}-1)\left[2\delta a_0^\varepsilon c_0^\varepsilon(t) + \frac{a(0)}{2}\delta \sum_{i=1}^{\lfloor \frac{1}{\sqrt{\varepsilon}}\rfloor} c_i^\varepsilon(t)\,\mathrm{e}^{-ix} - \mathrm{e}^{x} \sum_{i\ge \lfloor \frac{1}{\sqrt{\varepsilon}}\rfloor+1} b_i^\varepsilon c_i^\varepsilon(t)\,\mathrm{e}^{-ix}\right].$$

The term in c_0^ε and the first sum are combined and using our choice of δ, it yields :

$$2\delta a_0^\varepsilon c_0^\varepsilon(t) + \frac{a(0)}{2}\delta \sum_{i=1}^{\lfloor \frac{1}{\sqrt{\varepsilon}}\rfloor} c_i^\varepsilon(t)\,\mathrm{e}^{-ix} \ge \frac{a(0)}{2}\delta\left(H^\varepsilon(t,x) - \sum_{i\ge \lfloor \frac{1}{\sqrt{\varepsilon}}\rfloor+1} c_i^\varepsilon(t)\,\mathrm{e}^{-ix}\right).$$

Hence :

$$\varepsilon\partial_t H^\varepsilon(t,x) \le (1-\mathrm{e}^{-x}) \quad \left[\frac{a(0)}{2}\delta\left(-H^\varepsilon(t,x) + \sum_{i\ge \lfloor \frac{1}{\sqrt{\varepsilon}}\rfloor+1} c_i^\varepsilon(t)\,\mathrm{e}^{-ix}\right) + \mathrm{e}^{x} \sum_{i\ge \lfloor \frac{1}{\sqrt{\varepsilon}}\rfloor+1} b_i^\varepsilon c_i^\varepsilon(t)\,\mathrm{e}^{-ix}\right].$$

Observe that for ε small enough depending on x, for all $i \ge \lfloor \frac{1}{\sqrt{\varepsilon}}\rfloor$, we have :

$$(\delta\frac{a(0)}{2} + \mathrm{e}^{x}\, b_i^\varepsilon)\,\mathrm{e}^{-ix} \le K(C_a+C_b)(1+i\varepsilon)\,\mathrm{e}^{-ix} \le K\varepsilon,$$

which leads to :

$$\varepsilon\partial_t H^\varepsilon(t,x) \le \frac{a(0)}{2}\delta(\mathrm{e}^{-x}-1)H^\varepsilon(t,x) + (1-\mathrm{e}^{-x})Km.$$

We conclude by using Grönwall's lemma and $\tilde{K} = \frac{2Km}{\delta a(0)}$ and (23) follows immediately. □

A direct consequence of Lemma 3.2 is the following refined estimate on c_0^ε which shows that at the limit $\varepsilon \to 0$, the density f^ε vanishes at the boundary, in agreement with the limiting boundary condition (11c):

Lemma 3.3. *There exist constants $C_1, C_2 > 0$ such that for ε small enough and for all $t \in (0,T]$:*

$$c_0^\varepsilon(t) \le \mathrm{e}^{-\frac{C_1}{\varepsilon}t}\, c_0^{\varepsilon,0} + \varepsilon C_2. \tag{26}$$

Proof. As in the proof of Lemma 3.2, there exists ε small enough such that :

$$\frac{\mathrm{d}c_0^\varepsilon(t)}{\mathrm{d}t} = \frac{1}{\varepsilon}(b_1^\varepsilon c_1^\varepsilon(t) - a_0^\varepsilon \frac{L^\varepsilon(t)}{L^\varepsilon(t)+\kappa} c_0^\varepsilon(t)) \le C_b\bar{c_1} - \frac{a(0)}{\varepsilon}\delta c_0^\varepsilon(t),$$

thanks to hypothesis (H'1). Now applying Grönwall's lemma, we obtain :

$$c_0^\varepsilon(t) \le \mathrm{e}^{-\frac{a(0)\delta t}{\varepsilon}}\, c_0^\varepsilon(0) + C_b\bar{c_1}\frac{\varepsilon}{\delta a(0)}(1-\mathrm{e}^{-\frac{a(0)}{\varepsilon}\delta t}),$$

which gives the desired result. □

We end this section by a last lemma that will be useful to control the first spatial derivative of F^ε.

Lemma 3.4. *We have, for all $T > 0$, and for ε small enough,*

$$\sup_{t\le T}\sum_{i\ge 0}|c_{i+1}^\varepsilon - c_i^\varepsilon|(t) < \infty, \tag{27}$$

$$\sup_{t\le T}\varepsilon\sum_{i\ge 0} i|c_{i+1}^\varepsilon - c_i^\varepsilon|(t) < \infty. \tag{28}$$

Proof. Let $u_i = c_{i+1}^\varepsilon - c_i^\varepsilon$ and let's estimate its time derivative. Then, for all $i \ge 1$, we have from Eq.(13) and Eq.(12):

$$\begin{aligned}
\frac{\mathrm{d}u_i}{\mathrm{d}t} =& \frac{L^\varepsilon(t)}{L^\varepsilon(t)+\kappa}\left(\frac{a_{i-1}^\varepsilon}{\varepsilon}u_{i-1} - \frac{a_{i-1}^\varepsilon - a_i^\varepsilon}{\varepsilon}c_i^\varepsilon - \frac{a_i^\varepsilon}{\varepsilon}u_i - \frac{a_{i+1}^\varepsilon - a_i^\varepsilon}{\varepsilon}c_{i+1}^\varepsilon\right)\\
&- \left(\frac{b_i^\varepsilon}{\varepsilon}u_i - \frac{b_{i+1}^\varepsilon + b_i^\varepsilon}{\varepsilon}c_{i+1}^\varepsilon - \frac{b_{i+1}^\varepsilon}{\varepsilon}u_{i+1} + \frac{b_{i+1}^\varepsilon - b_{i+2}^\varepsilon}{\varepsilon}c_{i+2}^\varepsilon\right)\\
=& \frac{J_{i-1}^\varepsilon(u,L^\varepsilon) - J_i^\varepsilon(u,L^\varepsilon)}{\varepsilon} + \frac{L^\varepsilon(t)}{L^\varepsilon(t)+\kappa}\left(\frac{a_{i-1}^\varepsilon - a_i^\varepsilon}{\varepsilon}u_i - \left(\frac{a_{i-1}^\varepsilon - a_i^\varepsilon}{\varepsilon} + \frac{a_{i+1}^\varepsilon - a_i^\varepsilon}{\varepsilon}\right)c_{i+1}^\varepsilon\right)\\
&+ \frac{b_{i+1}^\varepsilon - b_i^\varepsilon}{\varepsilon}u_{i+1} + \left(\frac{b_{i+1}^\varepsilon - b_i^\varepsilon}{\varepsilon} + \frac{b_{i+1}^\varepsilon - b_{i+2}^\varepsilon}{\varepsilon}\right)c_{i+2}^\varepsilon.
\end{aligned}$$

We multiply the previous expression for $i \ge 1$ by $\mathrm{sign}(u_i)$ on both sides, which gives :

$$\begin{aligned}
\frac{\mathrm{d}|u_i|}{\mathrm{d}t} \le& \frac{J_{i-1}^\varepsilon(|u|,L^\varepsilon) - J_i^\varepsilon(|u|,L^\varepsilon)}{\varepsilon} + \frac{|a_{i-1}^\varepsilon - a_i^\varepsilon|}{\varepsilon}|u_i| + \frac{|a_{i-1}^\varepsilon - 2a_i^\varepsilon + a_{i+1}^\varepsilon|}{\varepsilon}c_{i+1}^\varepsilon\\
&+ \frac{|b_{i+1}^\varepsilon - b_i^\varepsilon|}{\varepsilon}|u_{i+1}| + \frac{|b_{i+2}^\varepsilon - 2b_{i+1}^\varepsilon + b_i^\varepsilon|}{\varepsilon}c_{i+2}^\varepsilon.
\end{aligned}$$

Hence, thanks to hypotheses (H3) and (H5) and Lemma 3.2, there exists ε small enough such that for $i \ge 1$:

$$\frac{\mathrm{d}|u_i|}{\mathrm{d}t} \le \frac{J_{i-1}^\varepsilon(|u|,L^\varepsilon) - J_i^\varepsilon(|u|,L^\varepsilon)}{\varepsilon} + \|a'\|_\infty|u_i| + \varepsilon\|a''\|_\infty c_{i+1}^\varepsilon + \|b'\|_\infty|u_{i+1}| + \varepsilon\|b''\|_\infty c_{i+2}^\varepsilon. \tag{29}$$

Now, for $i = 0$, we obtain :

$$\frac{\mathrm{d}u_0}{\mathrm{d}t} = -\frac{1}{\varepsilon}J_0^\varepsilon(u,L^\varepsilon) - \frac{a_1^\varepsilon - a_0^\varepsilon}{\varepsilon}\frac{L^\varepsilon(t)}{L^\varepsilon(t)+\kappa}c_1^\varepsilon + \frac{a_0^\varepsilon}{\varepsilon}\frac{L^\varepsilon(t)}{L^\varepsilon(t)+\kappa}c_0^\varepsilon + \frac{b_2^\varepsilon - b_1^\varepsilon}{\varepsilon}c_2^\varepsilon - \frac{b_1^\varepsilon}{\varepsilon}c_1^\varepsilon.$$

Since $b_0^\varepsilon = b(0) = 0$, we can treat the remaining terms in b as before by adding and removing the right terms for free. The terms with c_1^ε are bounded using Lemma 3.2 and the one with c_0^ε using Lemma 3.3. Hence, there exists ε small enough such that :

$$\frac{\mathrm{d}|u_0|}{\mathrm{d}t} \le -\frac{1}{\varepsilon}J_0^\varepsilon(|u|,L^\varepsilon) + \|a'\|_\infty\bar{c_1} + \frac{a(0)}{\varepsilon}\,\mathrm{e}^{-\frac{C_1}{\varepsilon}t}\,c_0^{\varepsilon,0} + a(0)C_2 + \|b'\|_\infty|u_1| + \varepsilon\|b''\|_\infty c_2^\varepsilon.$$

We sum the previous estimates for all $i \ge 0$ and we get :

$$\frac{\mathrm{d}}{\mathrm{d}t}\sum_{i\ge 0}|u_i| \le (\|a'\|_\infty + \|b'\|_\infty)\sum_{i\ge 0}|u_i| + (\|a''\|_\infty + \|b''\|_\infty)\varepsilon\sum_{i\ge 0}c_i^\varepsilon + \|a'\|_\infty\bar{c_1} + \frac{a(0)}{\varepsilon}\,\mathrm{e}^{-\frac{C_1}{\varepsilon}t}\,c_0^{\varepsilon,0} + a(0)C_2.$$

We integrate the previous inequality over $[0,t]$, for $0<t<T$:

$$\sum_{i\geq 0}|u_i|(t) \leq \sum_{i\geq 0}|u_i|(0) + (\|a'\|_\infty + \|b'\|_\infty)\int_0^t \sum_{i\geq 0}|u_i|(s)\mathrm{d}s \\ + (\|a''\|_\infty + \|b''\|_\infty)mT + \frac{a(0)}{C_1}c_0^{\varepsilon,0} + (a(0)C_2 + \|a'\|_\infty \bar{c_1})T.$$

And finally Grönwall's lemma yields :

$$\sum_{i\geq 0}|u_i|(t) \leq C_u(T)$$

with

$$C_u(T) = \left(\sum_{i\geq 0}|u_i|(0) + (\|a''\|_\infty + \|b''\|_\infty)mT + \frac{a(0)}{C_1}c_0^{\varepsilon,0} + (a(0)C_2 + \|a'\|_\infty \bar{c_1})T\right) \\ \times \exp((\|a'\|_\infty + \|b'\|_\infty)T),$$

which gives Eq. (27).

Using the definition (13c) of λ, estimate (29) and hypothesis (H'1), we obtain the following inequalities :

$$\begin{aligned}\varepsilon\frac{\mathrm{d}}{\mathrm{d}t}\sum_{i\geq 1} i|u_i| &\leq \varepsilon\sum_{i\geq 1} i\frac{J_{i-1}^\varepsilon(|u|) - J_i^\varepsilon(|u|)}{\varepsilon} + \varepsilon(\|a'\|_\infty + \|b'\|_\infty)\sum_{i\geq 1} i|u_i| + (\|a''\|_\infty + \|b''\|_\infty)\varepsilon^2\sum_{i\geq 0} ic_i^\varepsilon \\ &\leq \sum_{i\geq 0} J_i^\varepsilon(|u|) + (\|a'\|_\infty + \|b'\|_\infty)\varepsilon\sum_{i\geq 1} i|u_i| + (\|a''\|_\infty + \|b''\|_\infty)\lambda \\ &\leq C_a\sum_{i\geq 0}|u_i| + (\|a'\|_\infty + \|b'\|_\infty)\varepsilon\sum_{i\geq 1} i|u_i| + (\|a''\|_\infty + \|b''\|_\infty)\lambda.\end{aligned}$$

Integrating over $[0,t]$ and using the previous bound on $\sum_{i\geq 0}|u_i|$, we conclude using Grönwall's lemma :

$$\varepsilon\sum_{i\geq 1} i|u_i|(t) \leq \left(\varepsilon\sum_{i\geq 1} i|u_i|(0) + C_aC_u(T)T + (\|a''\|_\infty + \|b''\|_\infty)\lambda T\right)\exp((\|a'\|_\infty + \|b'\|_\infty)T),$$

which yields Eq. (28). □

3.2 Proof of theorem 3.1

In this section, we make use of the lemmas from the previous section. As such, from then on, ε is taken small enough to apply those lemmas. We first derive the equation satisfied by the tail distribution F^ε defined at Eq.(20). Recall that operator Δ_ε is defined at Eq.(19).

Lemma 3.5. *For all $x \geq \frac{\varepsilon}{2}$ and $t \geq 0$:*

$$\partial_t F^\varepsilon(t,x) = -\frac{1}{\varepsilon}\int_{x-\varepsilon}^{x}(a^\varepsilon(y)\frac{L^\varepsilon(t)}{L^\varepsilon(t)+\kappa} - a(x)\frac{L(t)}{L(t)+\kappa})f^\varepsilon(t,y)\mathrm{d}y - a(x)\frac{L(t)}{L(t)+\kappa}\Delta_{-\varepsilon}F^\varepsilon(t,x) + \frac{1}{\varepsilon}\int_{x}^{x+\varepsilon}(b^\varepsilon(y)-b(x))f^\varepsilon(t,y)\mathrm{d}y + b(x)\Delta_\varepsilon F^\varepsilon(t,x) \quad (30)$$

and for all $x < \frac{\varepsilon}{2}$ and $t \geq 0$:

$$\partial_t F^\varepsilon(t,x) = \frac{1}{\varepsilon}\int_{-\frac{\varepsilon}{2}}^{x} a^\varepsilon(y)\frac{L^\varepsilon(t)}{L^\varepsilon(t)+\kappa}f^\varepsilon(t,y)\mathrm{d}y - \frac{1}{\varepsilon}\int_{\frac{\varepsilon}{2}}^{x+\varepsilon} b^\varepsilon(y)f^\varepsilon(t,y)\mathrm{d}y. \quad (31)$$

Remark. *The function f^ε is defined on $[-\frac{\varepsilon}{2},+\infty[$ whereas f is defined on $\mathbb{R}_+$. However we will only concern ourselves with $x \in \mathbb{R}_+$ in the following subsections. Hence we will treat the case $x < \varepsilon/2$ independently to accommodate for boundary terms that might be left off from f^ε. We also point out that :*

$$\int_0^{+\infty} f^\varepsilon(t,x)\mathrm{d}x = m - \frac{\varepsilon}{2}c_0^\varepsilon(t) \quad (32)$$

Owing to Lemma 3.2, the right hand side is bounded and tends to m as $\varepsilon \to 0$.And for the first order we have an exact computation :

$$L^\varepsilon(t) + \int_0^{+\infty} x f^\varepsilon(t,x)\mathrm{d}x = \lambda \quad (33)$$

Proof. For all $x \in \mathbb{R}_+$ and $t \in [0,T]$, it comes directly from the definitions (19) and (20) that the following equations hold true :

for all $x \geq 0$ and $t \geq 0$,

$$\Delta_\varepsilon F^\varepsilon(t,x) = -\frac{1}{\varepsilon}\int_x^{x+\varepsilon} f^\varepsilon(t,y)\mathrm{d}y, \quad (34)$$

and for all $x \geq \frac{\varepsilon}{2}$ and $t \geq 0$,

$$\Delta_{-\varepsilon} F^\varepsilon(t,x) = -\frac{1}{\varepsilon}\int_{x-\varepsilon}^{x} f^\varepsilon(t,y)\mathrm{d}y. \quad (35)$$

Denote $H_x = \mathbb{1}_{[x,+\infty)}$. First observe that :

$$\Delta_\varepsilon H_x(y) = \frac{1}{\varepsilon}\left(\mathbb{1}_{[x,+\infty)}(y+\varepsilon) - \mathbb{1}_{[x,+\infty)}(y)\right) = \frac{1}{\varepsilon}\mathbb{1}_{[x-\varepsilon,x)}(y),$$

$$\Delta_{-\varepsilon} H_x(y) = \frac{1}{\varepsilon}\mathbb{1}_{[x,x+\varepsilon)}(y).$$

Then we use Proposition 2.2 for the Heaviside function. It yields that for all $x \geq \frac{\varepsilon}{2}$:

$$
\begin{aligned}
\partial_t F^\varepsilon(t,x) &= \int_{\mathbb{R}_+} H_x(y)\partial_t f^\varepsilon(t,y)\mathrm{d}y \\
&= \int_{\mathbb{R}_+} \left(\Delta_\varepsilon H_x(y)a^\varepsilon(y)\frac{L^\varepsilon(t)}{L^\varepsilon(t)+\kappa} - \Delta_{-\varepsilon}H_x(y)b^\varepsilon(y)\right) f^\varepsilon(t,y)\mathrm{d}y \\
&= \int_{x-\varepsilon}^{x} \frac{1}{\varepsilon}a^\varepsilon(y)\frac{L^\varepsilon(t)}{L^\varepsilon(t)+\kappa} f^\varepsilon(t,y)\mathrm{d}y - \int_x^{x+\varepsilon}\frac{1}{\varepsilon}b^\varepsilon(y)f^\varepsilon(t,y)\mathrm{d}y \\
&= \frac{1}{\varepsilon}\int_{x-\varepsilon}^{x}(a^\varepsilon(y)\frac{L^\varepsilon(t)}{L^\varepsilon(t)+\kappa} - a(x)\frac{L(t)}{L(t)+\kappa})f^\varepsilon(t,y)\mathrm{d}y - a(x)\frac{L(t)}{L(t)+\kappa}\Delta_{-\varepsilon}F^\varepsilon(t,x) \\
&- \frac{1}{\varepsilon}\int_x^{x+\varepsilon}(b^\varepsilon(y)-b(x))f^\varepsilon(t,y)\mathrm{d}y + b(x)\Delta_\varepsilon F^\varepsilon(t,x)
\end{aligned}
$$

The case for $x < \frac{\varepsilon}{2}$ follows from simple computation, using that $\int_{-\varepsilon/2}^{+\infty} f^\varepsilon(t,x)\mathrm{d}x = m$ by conservation of the moment (14) :

$$
\begin{aligned}
\partial_t F^\varepsilon(t,x) &= \frac{\mathrm{d}}{\mathrm{d}t}\int_{\frac{-\varepsilon}{2}}^{+\infty} f^\varepsilon(t,y)\mathrm{d}y - \frac{\mathrm{d}}{\mathrm{d}t}\int_{\frac{-\varepsilon}{2}}^{x} f^\varepsilon(t,y)\mathrm{d}y = -(x+\frac{\varepsilon}{2})\frac{\mathrm{d}}{\mathrm{d}t}c_0^\varepsilon(t) \\
&= \frac{1}{\varepsilon}\int_{\frac{-\varepsilon}{2}}^{x} a^\varepsilon(y)\frac{L^\varepsilon(t)}{L^\varepsilon(t)+\kappa}f^\varepsilon(t,y)\mathrm{d}y - \frac{1}{\varepsilon}\int_{\frac{\varepsilon}{2}}^{x+\varepsilon} b^\varepsilon(y)f^\varepsilon(t,y)\mathrm{d}y.
\end{aligned}
$$

□

We then derive an upper bound for the time derivative of $\int_{\mathbb{R}_+}|E(t,x)|\mathrm{d}x$, where E is defined at Eq.(21).

Lemma 3.6. *For all $t \geq 0$, we have :*

$$
\begin{aligned}
\frac{d}{\mathrm{d}t}\int_{\mathbb{R}_+}|E(t,x)|\mathrm{d}x \leq (\|a'\|_\infty + \|b'\|_\infty)\int_{\mathbb{R}_+}|E(t,x)|\mathrm{d}x + \int_{\mathbb{R}_+}|\partial_t F^\varepsilon(t,x) + v(x,L(t))\partial_x F^\varepsilon(t,x)|\mathrm{d}x \\
+ \frac{\varepsilon}{2}a(0)\frac{L(t)}{L(t)+\kappa}c_0^\varepsilon(t).
\end{aligned} \tag{36}
$$

Proof. From the definitions of the tail distributions in Eq. (20), the following equations hold true :

$$
\partial_x F(t,x) = -f(t,x)\,,
$$

$$
\partial_x F^\varepsilon(t,x) = -f^\varepsilon(t,x), \text{ a.e. in } \mathbb{R}_+\,.
$$

By Def.2.3, we have :

$$
F(t,x) = \int_{\max(x,X_c(t))}^{+\infty} f^0(X(0;t,y))\partial_y X(0;t,y)\mathrm{d}y = \begin{cases} \int_0^{+\infty} f^0(y)\mathrm{d}y & \text{if } x \leq X_c(t), \\ \int_{X(0;t,x)}^{+\infty} f^0(y)\mathrm{d}y & \text{if } x \geq X_c(t). \end{cases}
$$

Therefore if $x \leq X_c(t)$, then $\partial_t F(t,x) = 0 = \partial_x F(t,x)$. And if $x \geq X_c(t)$, the following expressions hold :

$$\partial_t F(t,x) = -f^0(X(0;t,x))\partial_t X(0;t,x),$$

$$\partial_x F(t,x) = -f^0(X(0;t,x))\partial_x X(0;t,x) = -f(t,x).$$

By properties of characteristics we have : $\partial_t X(0;t,x) + v(x,L)\partial_x X(0;t,x) = 0$ and thus :

$$\partial_t F(t,x) + v(x,L(t))\partial_x F(t,x) = -f^0(X(0;t,x))(\partial_t X(0;t,x) + v(x,L)\partial_x X(0;t,x)) = 0.$$

We then compute :

$$\begin{aligned}\partial_t E(t,x) &= \partial_t F^\varepsilon(t,x) - \partial_t F(t,x)\\ &= -v(x,L(t))\partial_x(F^\varepsilon - F)(t,x) + \partial_t F^\varepsilon(t,x) + v(x,L(t))\partial_x F^\varepsilon(t,x).\end{aligned}$$

We integrate the previous equality, we use the definition (3) of v with hypothesis (H3) and we find :

$$\begin{aligned}\frac{\mathrm{d}}{\mathrm{d}t}\int_{\mathbb{R}_+}|E|\mathrm{d}x &= -\int_{\mathbb{R}_+} v\partial_x|E|\mathrm{d}x + \int_{\mathbb{R}_+}\mathrm{sign}(E)(\partial_t F^\varepsilon + v(x,L(t))\partial_x F^\varepsilon)\mathrm{d}x\\ &= -[v(x,L(t))|E(t,x)|]_0^{+\infty} + \int_{\mathbb{R}_+}\partial_x v|E|\mathrm{d}x + \int_{\mathbb{R}_+}\mathrm{sign}(E)(\partial_t F^\varepsilon + v\partial_x F^\varepsilon)\mathrm{d}x\\ &\leq v(0,L(t))|E(t,0)| + (\|a'\|_\infty + \|b'\|_\infty)\int_{\mathbb{R}_+}|E|\mathrm{d}x + \int_{\mathbb{R}_+}|\partial_t F^\varepsilon + v\partial_x F^\varepsilon|\mathrm{d}x\\ &= (\|a'\|_\infty + \|b'\|_\infty)\int_{\mathbb{R}_+}|E|\mathrm{d}x + \int_{\mathbb{R}_+}|\partial_t F^\varepsilon + v\partial_x F^\varepsilon|\mathrm{d}x + \frac{\varepsilon}{2}a(0)\frac{L(t)}{L(t)+\kappa}c_0^\varepsilon(t).\end{aligned}$$

The last equality is obtained since $b(0) = 0$ and $|E(t,0)| = |\int_{\mathbb{R}_+}(f^\varepsilon - f)(t,x)\mathrm{d}x| = \frac{\varepsilon}{2}c_0^\varepsilon(t)$, see Eq.(32). □

Thanks to the equation on F^ε given by Lemma 3.5, we control the second term in Eq. (36) in the next lemma.

Lemma 3.7. *There exist some constants $C_1, C_2 > 0$ independent of ε such that for all $t \in [0,T]$:*

$$\int_{\mathbb{R}_+}|(\partial_t F^\varepsilon + v\partial_x F^\varepsilon)(t,x)|\mathrm{d}x \leq \varepsilon C_1 + C_2|L^\varepsilon(t) - L(t)|. \tag{37}$$

Proof. First by construction of both a^ε and b^ε, and the fact that a and b are lipshitz continuous, one has for all $x, y \in \mathbb{R}_+$ such that $|y - x| \leq \varepsilon$:

$$|\frac{a^\varepsilon(y) - a(x)}{\varepsilon}| \leq 2\|a'\|_\infty$$

and similarly for b^ε.

Then using equation (30) and definition (3) of v, we find the following estimate for all $x \geq \frac{\varepsilon}{2}$:

$$|\partial_t F^\varepsilon + v\partial_x F^\varepsilon| \le 2\|a'\|_\infty \int_{x-\varepsilon}^{x} f^\varepsilon + \frac{1}{\varepsilon}\frac{a(x)}{\kappa}|L^\varepsilon(t) - L(t)| \int_{x-\varepsilon}^{x} f^\varepsilon + 2\|b'\|_\infty \int_{x}^{x+\varepsilon} f^\varepsilon$$
$$+ a(x)\frac{L(t)}{L(t)+\kappa}|\partial_x F^\varepsilon - \Delta_{-\varepsilon} F^\varepsilon| + b(x)|\partial_x F^\varepsilon - \Delta_\varepsilon F^\varepsilon|.$$

Using equation (31), hypotheses (H'1) and (H2b) and Lemma 3.2, we find for all $x < \frac{\varepsilon}{2}$:

$$\begin{aligned}
|\partial_t F^\varepsilon + v\partial_x F^\varepsilon| &\le |\frac{1}{\varepsilon}\int_{-\frac{\varepsilon}{2}}^{x} a^\varepsilon(y)\frac{L^\varepsilon(t)}{L^\varepsilon(t)+\kappa} f^\varepsilon(t,y)\mathrm{d}y - a(x)\frac{L(t)}{L(t)+\kappa} f^\varepsilon(t,x)| \\
&\quad + |\frac{1}{\varepsilon}\int_{\frac{\varepsilon}{2}}^{x+\varepsilon} b^\varepsilon(y) f^\varepsilon(t,y)\mathrm{d}y - b(x) f^\varepsilon(t,x)| \\
&\le |\frac{x+\frac{\varepsilon}{2}}{\varepsilon} a(0)\frac{L^\varepsilon(t)}{L^\varepsilon(t)+\kappa} c_0^\varepsilon(t) - a(x)\frac{L(t)}{L(t)+\kappa} c_0^\varepsilon(t)| + |\frac{x+\frac{\varepsilon}{2}}{\varepsilon} b_1^\varepsilon c_1^\varepsilon(t) - b(x) c_0^\varepsilon(t)| \\
&\le a(0)c_0^\varepsilon(t)\frac{x+\frac{\varepsilon}{2}}{\varepsilon}\frac{1}{\kappa}|L^\varepsilon(t) - L(t)| + |a(x) - \frac{x+\frac{\varepsilon}{2}}{\varepsilon}a(0)|c_0^\varepsilon(t) + C_b\varepsilon c_1^\varepsilon(t) + C_b\frac{\varepsilon}{2}c_0^\varepsilon(t) \\
&\le a(0)\bar{c_0}\frac{1}{\kappa}|L^\varepsilon(t) - L(t)| + (a(0) + \frac{\varepsilon}{2}\|a'\|_\infty)\bar{c_0} + C_b\bar{c_1}\varepsilon + C_b\frac{\varepsilon}{2}\bar{c_0}.
\end{aligned}$$

Now we can integrate $|\partial_t F^\varepsilon + v\partial_x F^\varepsilon|$ over $\mathbb{R}_+$ using the two previous estimates. Note that using Fubini's theorem and Eq.(32), we have

$$\begin{aligned}
\int_{\frac{\varepsilon}{2}}^{+\infty}\int_{x-\varepsilon}^{x} f^\varepsilon(y)\mathrm{d}y\mathrm{d}x &= \int_{-\frac{\varepsilon}{2}}^{+\infty} f^\varepsilon(t,y)\int_{\max(y,\varepsilon/2)}^{y+\varepsilon}\mathrm{d}x\mathrm{d}y = \varepsilon\int_{\frac{\varepsilon}{2}}^{+\infty} f^\varepsilon(t,y)\mathrm{d}y + \frac{\varepsilon^2}{2}c_0^\varepsilon(t) \\
&= \int_0^{+\infty} f^\varepsilon(t,y)\mathrm{d}y \le \varepsilon m.
\end{aligned}$$

Therefore, we get :

$$\begin{aligned}
\int_{\mathbb{R}_+}|\partial_t F^\varepsilon + v\partial_x F^\varepsilon|\mathrm{d}x &\le \varepsilon(2\|a'\|_\infty + 2\|b'\|_\infty|)m + \frac{\|a\|_\infty}{\kappa}|L^\varepsilon(t) - L(t)|m \\
&\quad + \|a\|_\infty\frac{L(t)}{L(t)+\kappa}\int_{\frac{\varepsilon}{2}}^{+\infty}|\partial_x F^\varepsilon - \Delta_{-\varepsilon}F^\varepsilon|\mathrm{d}x + \int_{\frac{\varepsilon}{2}}^{+\infty} b(x)|\partial_x F^\varepsilon - \Delta_\varepsilon F^\varepsilon|\mathrm{d}x \\
&\quad + \frac{\varepsilon}{2}(a(0)\bar{c_0}\frac{1}{\kappa}|L^\varepsilon(t) - L(t)| + (a(0) + \frac{\varepsilon}{2}\|a'\|_\infty)\bar{c_0} + C_b\bar{c_1}\varepsilon + C_b\frac{\varepsilon}{2}\bar{c_0}).
\end{aligned} \tag{38}$$

We now compute the difference between the continuous and discrete derivatives on F^ε. We denote by $\lfloor x \rceil$ the nearest integer function with the upper-rounding convention : $\lfloor 0.5 \rceil = 1$. Figure 2 shows a representation of the cells Γ_{i-1}^ε, Γ_i^ε and Γ_{i+1}^ε as well as an example of the result of $\lfloor \frac{x}{\varepsilon} \rceil$ for $x \in \Gamma_i^\varepsilon$.

Let us first compute the integral of $|\partial_x F^\varepsilon - \Delta_{-\varepsilon}F^\varepsilon|$, using Eq.(35) and the fact that f^ε is constant

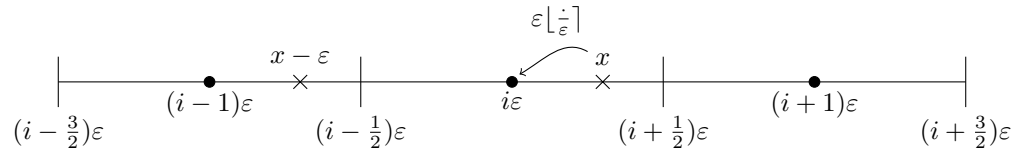

Figure 2: Representation of the cells Γ_{i-1}^ε, Γ_i^ε and Γ_{i+1}^ε and of the value $\varepsilon\lfloor\frac{x}{\varepsilon}\rceil$.

equal to $c_i^\varepsilon(t)$ on the cells Γ_i^ε :

$$\begin{aligned}\int_{\frac{\varepsilon}{2}}^{+\infty}|\partial_x F^\varepsilon-\Delta_{-\varepsilon}F^\varepsilon|\mathrm{d}x &= \int_{\frac{\varepsilon}{2}}^{+\infty}|f^\varepsilon(t,x)-\frac{1}{\varepsilon}\int_{x-\varepsilon}^{x}f^\varepsilon(t,y)\mathrm{d}y|\mathrm{d}x\\ &= \int_{\frac{\varepsilon}{2}}^{+\infty}\frac{1}{\varepsilon}|\int_{x-\varepsilon}^{x}(f^\varepsilon(t,x)-f^\varepsilon(t,y))\mathrm{d}y|\mathrm{d}x\\ &= \int_{\frac{\varepsilon}{2}}^{+\infty}\frac{1}{\varepsilon}|\int_{x-\varepsilon}^{\varepsilon(\lfloor\frac{x}{\varepsilon}\rceil-\frac{1}{2})}(f^\varepsilon(t,x)-f^\varepsilon(t,y))\mathrm{d}y|\mathrm{d}x\\ &= \int_{\frac{\varepsilon}{2}}^{+\infty}|c^\varepsilon_{\lfloor\frac{x}{\varepsilon}\rceil}(t)-c^\varepsilon_{\lfloor\frac{x}{\varepsilon}\rceil-1}(t)|\frac{\varepsilon(\lfloor\frac{x}{\varepsilon}\rceil-\frac{1}{2})-(x-\varepsilon)}{\varepsilon}\mathrm{d}x.\end{aligned}$$

Now, observe that for all $x\in\Gamma_i^\varepsilon$ one has $c^\varepsilon_{\lfloor\frac{x}{\varepsilon}\rceil}(t)-c^\varepsilon_{\lfloor\frac{x}{\varepsilon}\rceil-1}(t)=c_i^\varepsilon(t)-c_{i-1}^\varepsilon(t)$, which gives :

$$\begin{aligned}\int_{\frac{\varepsilon}{2}}^{+\infty}|\partial_x F^\varepsilon-\Delta_{-\varepsilon}F^\varepsilon|\mathrm{d}x &= \sum_{i\geq 1}|c_i^\varepsilon(t)-c_{i-1}^\varepsilon(t)|\int_{\Gamma_i^\varepsilon}\frac{\varepsilon(\lfloor\frac{x}{\varepsilon}\rceil-\frac{1}{2})-(x-\varepsilon)}{\varepsilon}\mathrm{d}x\\ &= \frac{\varepsilon}{2}\sum_{i\geq 1}|c_i^\varepsilon(t)-c_{i-1}^\varepsilon(t)|.\end{aligned}$$

Hence, according to Lemma 3.4 there exists a constant $C(T)>0$ independent of ε such that :

$$\int_{\frac{\varepsilon}{2}}^{+\infty}|\partial_x F^\varepsilon-\Delta_{-\varepsilon}F^\varepsilon|\mathrm{d}x\leq\varepsilon C(T). \tag{39}$$

We proceed similarly for the term $\int_{\mathbb{R}_+}b(x)|\partial_x F^\varepsilon-\Delta_\varepsilon F^\varepsilon|\mathrm{d}x$:

$$\begin{aligned}\int_{\frac{\varepsilon}{2}}^{\infty}b(x)|f^\varepsilon(t,x)-\frac{1}{\varepsilon}\int_{x}^{x+\varepsilon}f^\varepsilon(t,y)\mathrm{d}y|\mathrm{d}x &= \int_{\frac{\varepsilon}{2}}^{\infty}\frac{b(x)}{\varepsilon}|\int_{x}^{x+\varepsilon}(f^\varepsilon(t,x)-f^\varepsilon(t,y))\mathrm{d}y|\mathrm{d}x\\ &= \int_{\frac{\varepsilon}{2}}^{\infty}\frac{b(x)}{\varepsilon}|\int_{\varepsilon(\lfloor\frac{x}{\varepsilon}\rceil+\frac{1}{2})}^{x+\varepsilon}(f^\varepsilon(t,x)-f^\varepsilon(t,y))\mathrm{d}y|\mathrm{d}x\\ &= \int_{\frac{\varepsilon}{2}}^{\infty}|c^\varepsilon_{\lfloor\frac{x}{\varepsilon}\rceil+1}(t)-c^\varepsilon_{\lfloor\frac{x}{\varepsilon}\rceil}(t)|b(x)\frac{x-\varepsilon(\lfloor\frac{x}{\varepsilon}\rceil-\frac{1}{2})}{\varepsilon}\mathrm{d}x\\ &= \sum_{i\geq 1}|c_{i+1}^\varepsilon(t)-c_i^\varepsilon(t)|\int_{\Gamma_i^\varepsilon}b(x)\frac{x-\varepsilon(\lfloor\frac{x}{\varepsilon}\rceil-\frac{1}{2})}{\varepsilon}\mathrm{d}x.\end{aligned}$$

Owing to hypothesis (H2b), we simply bound the last integral as follows :

$$\int_{\Gamma_i^\varepsilon} b(x)\frac{x-\varepsilon(\lfloor\frac{x}{\varepsilon}\rceil-\frac{1}{2})}{\varepsilon}\mathrm{d}x \le C_b\frac{\varepsilon^2}{2}(i+\frac{1}{6}).$$

Hence, according to Lemma 3.4, there exists a constant $C(T)>0$ independent of ε such that :

$$\int_{\frac{\varepsilon}{2}}^{+\infty} b(x)|\partial_x F^\varepsilon - \Delta_x F^\varepsilon|\mathrm{d}x < \frac{\varepsilon}{6}C(T)(1+\frac{\varepsilon}{2}). \tag{40}$$

We conclude from Eqs. (38)-(39)-(40) by regrouping together terms not depending on ε.

□

We now proceed with the proof of Theorem 3.1.

Proof of Theorem 3.1. Let $T>0$ and consider $t\in(0,T]$. We begin by integrating (36) over $[0,t]$, using Lemma 3.7 :

$$\begin{aligned}\int_{\mathbb{R}_+}|E(t,x)|\mathrm{d}x &\le \int_{\mathbb{R}_+}|E(0,x)|\mathrm{d}x + (\|a'\|_\infty+\|b'\|_\infty)\int_0^t\int_{\mathbb{R}_+}|E(s,x)|\mathrm{d}x\mathrm{d}s\\ &+\int_0^t\int_{\mathbb{R}_+}|\partial_t F^\varepsilon(s,x)+v(x,L(s))\partial_x F^\varepsilon(s,x)|\mathrm{d}x\mathrm{d}s+\frac{\varepsilon}{2}a(0)T\bar{c_0}\\ &\le \int_{\mathbb{R}_+}|E(0,x)|\mathrm{d}x + (\|a'\|_\infty+\|b'\|_\infty)\int_0^t\int_{\mathbb{R}_+}|E(s,x)|\mathrm{d}x\mathrm{d}s\\ &+\varepsilon TC_1 + C_2\int_0^t|L^\varepsilon(s)-L(s)|\mathrm{d}s+\frac{\varepsilon}{2}a(0)T\bar{c_0}.\end{aligned}$$

Then observe that :

$$\int_{\mathbb{R}_+}xf^\varepsilon(t,x)dx = \int_{\mathbb{R}_+}x\sum_{i\ge0}\mathbb{1}_{\Gamma_i^\varepsilon}(x)c_i^\varepsilon(t)\mathrm{d}x = \sum_{i\ge0}\int_{\Gamma_i^\varepsilon}x\mathrm{d}xc_i^\varepsilon(t) = \sum_{i\ge0}i\varepsilon^2c_i^\varepsilon(t).$$

Using conservation equations (13c) and (7) and Fubini's theorem, this leads to the bound :

$$|L^\varepsilon(t)-L(t)| = |\int_0^\infty x(f^\varepsilon(t,x)-f(t,x))\mathrm{d}x| = |\int_0^\infty(F^\varepsilon(t,x)-F(t,x))\mathrm{d}x| \le \int_{\mathbb{R}_+}|E(t,x)|\mathrm{d}x,$$

which finally yields :

$$\begin{aligned}|L^\varepsilon(t)-L(t)|+\int_{\mathbb{R}_+}|E(t,x)|\mathrm{d}x &\le 2\int_{\mathbb{R}_+}|E(0,x)|\mathrm{d}x+2(\|a'\|_\infty+\|b'\|_\infty)\int_0^t\int_{\mathbb{R}_+}|E(s,x)|\mathrm{d}x\mathrm{d}s\\ &+2\varepsilon TC_1+2C_2\int_0^t|L^\varepsilon(s)-L(s)|\mathrm{d}s+\varepsilon a(0)T\bar{c_0}.\end{aligned}$$

By the assumption on $E(0,x)$ and Grönwall's lemma, we finally conclude that :

$$|L^\varepsilon(t)-L(t)|+\int_{\mathbb{R}_+}|E(t,x)|\mathrm{d}x \le \varepsilon\Big(2C_{\text{init}}+2C_1T+a(0)T\bar{c_0}\Big)\exp(2(\|a'\|_\infty+\|b'\|_\infty+C_2)T).$$

□

4 Derivation of second order model and stationary solutions

4.1 A second-order Lifshitz-Slyozov model with diffusion

Up to this point we have studied a Lifshitz-Slyozov model, that is to say a transport PDE. However, this model leads to stationary solutions which are combinations of Dirac masses centered at the zeros of velocity v. Hence, since we aim at obtaining asymptotically bimodal distributions, we would like to add a diffusion term to our model in order to smooth the stationary solutions. Unfortunately and up to our knowledge, no biological argument can be found to explain such a diffusive term or to give a proper way of deriving it from biological considerations. Nonetheless, one can see this diffusive term as a second order term emerging from the preceding convergence result, see for example [39], [34], [10].

We follow here the derivation of the diffusive term presented in [39] and we use the notation introduced at Section 3.

Now, from Proposition 2.2, we can add and subtract the appropriate terms in ϕ to get :

$$\begin{aligned}
\int_0^\infty (f^\varepsilon(t,x) - f^\varepsilon(0,x))\phi(x)\mathrm{d}x &= \int_0^t \int_0^\infty (\Delta_\varepsilon \phi(x) a^\varepsilon(x) \frac{L^\varepsilon(t)}{L^\varepsilon(t)+\kappa} - \Delta_{-\varepsilon}\phi(x) b^\varepsilon(x)) f^\varepsilon(t,x)\mathrm{d}x\mathrm{d}t \\
&= \int_0^t \int_0^\infty \frac{\phi(x+\varepsilon)-\phi(x-\varepsilon)}{2\varepsilon}(a^\varepsilon(x)\frac{L^\varepsilon(t)}{L^\varepsilon(t)+\kappa} - b^\varepsilon(x)) f^\varepsilon(t,x)\mathrm{d}x\mathrm{d}t \\
&+ \frac{\varepsilon}{2}\int_0^t \int_0^\infty \frac{\phi(x+\varepsilon)-2\phi(x)+\phi(x-\varepsilon)}{\varepsilon^2} a^\varepsilon(x)\frac{L^\varepsilon(t)}{L^\varepsilon(t)+\kappa} f^\varepsilon(t,x)\mathrm{d}x\mathrm{d}t \\
&+ \frac{\varepsilon}{2}\int_0^t \int_0^\infty \frac{\phi(x+\varepsilon)-2\phi(x)+\phi(x-\varepsilon)}{\varepsilon^2} b^\varepsilon(x) f^\varepsilon(t,x)\mathrm{d}x\mathrm{d}t \\
&= \int_0^t \int_0^\infty \bar{\Delta}_\varepsilon \phi(x)(a^\varepsilon(x)\frac{L^\varepsilon(t)}{L^\varepsilon(t)+\kappa} - b^\varepsilon(x)) f^\varepsilon(t,x)\mathrm{d}x\mathrm{d}t \\
&+ \frac{\varepsilon}{2}\int_0^t \int_0^\infty \Delta_\varepsilon^2 \phi(x)(a^\varepsilon(x)\frac{L^\varepsilon(t)}{L^\varepsilon(t)+\kappa} + b^\varepsilon(x)) f^\varepsilon(t,x)\mathrm{d}x\mathrm{d}t
\end{aligned}$$

where $\bar{\Delta}_h\phi(x) = \frac{\phi(x+h)-\phi(x-h)}{2h}$ and $\Delta_h^2\phi(x) = \frac{\phi(x+h)-2\phi(x)+\phi(x-h)}{h^2}$.

This leads us to study the PDE (17).

4.2 Stationary solutions for the second-order Lifshitz-Slyozov model

In this section, we present the stationary solutions of system (11) without diffusion and system (17) with diffusion. We notice that stationary solutions are very different in nature from one model to the other. Eq.(11) does not yield nontrivial smooth stationary functions, and we rather expect stationary solutions to be linear combinations of Dirac masses, located at roots of the asymptotic velocity.

We can compute explicitly stationary solutions of system (17), namely :

$$\partial_t g = 0 \Longleftrightarrow \partial_x(vg) - \frac{\varepsilon}{2}\partial_x^2(dg) = 0.$$

Together with boundary conditions (16) this leads to stationary solutions denoted by $M_{L_{\text{stat}}}$, depending on stationary $L_{\text{stat}} \in \mathbb{R}_+$ under the form :

$$M_{L_{\text{stat}}}(x) = \frac{C(m, L_{\text{stat}})}{d(x, L_{\text{stat}})} \exp\Big(\frac{2}{\varepsilon}\int_0^x \frac{v(y, L_{\text{stat}})}{d(y, L_{\text{stat}})}\mathrm{d}y\Big), \tag{41}$$

where the constant $C(m, L_{\text{stat}})$ is determined in order to satisfy $\int_{\mathbb{R}_+} M_{L_{\text{stat}}}(t, x)\mathrm{d}x = m$, that is to say

$$C(m, L_{\text{stat}}) = \frac{m}{\displaystyle\int_{\mathbb{R}_+} \frac{1}{d(x, L_{\text{stat}})} \exp\Big(\frac{2}{\varepsilon}\int_0^x \frac{v(y, L_{\text{stat}})}{d(y, L_{\text{stat}})}\mathrm{d}y\Big)\mathrm{d}x}$$

and L_{stat} solves the constraint equation

$$L_{\text{stat}} + \int_{\mathbb{R}_+} x M_{L_{\text{stat}}}(x)\mathrm{d}x = \lambda. \tag{42}$$

Note that function $\Phi : L \to L + \displaystyle\int_{\mathbb{R}_+} x M_L(x)\mathrm{d}x$ is continuous on $\mathbb{R}_+$. Moreover, straightforward computations show that thanks to expression (41) and expressions for a and b that $\Phi(0) = 0$ and $\Phi \underset{L\to+\infty}{\to} +\infty$. Therefore, for all $\lambda \geq 0$, there exists at least one value for L which satisfies Eq.(42). Regarding unicity of stationary solutions, it would need to prove strict monotonicity of Φ, which is so far an open question. However, we may observe numerically that the application $\Phi : L \to L + \int_0^{x_{\max}} x M_L(x)\mathrm{d}x$ seems strictly non-decreasing, see Figure 3.

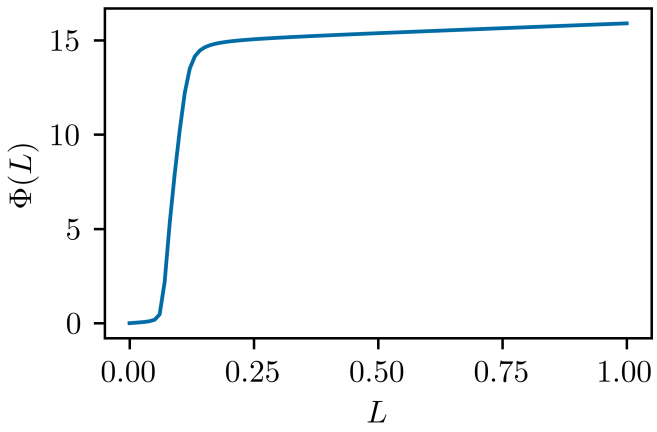

Figure 3: Plot of function $L \to \Phi(L)$ for $L \in [10^{-12}, 1]$ with functions a and b defined at Eq.(4) and (5) and parameters given at Table 1.

Remark. *In other modeling contexts, one may choose different functions a and b such that existence of stationary solutions may not be true for all value of λ. For example, $a(x) = 1$ and $b(x) = x^s$ with $s \leq 1$ implies $\lim\limits_{L\to 0^+} \Phi(L) = \lambda_0 > 0$. Hence for values of λ such that $\lambda < \lambda_0$, the system might not have smooth stationary solutions, see section 5.2.5 and Figures 14 and 15.*

In the following section, we will present some numerical simulations for system (17) and control that stationary solutions $M_{L_{\text{stat}}}$ follow a bimodal distribution for well-chosen parameters.

5 Numerical simulations

In this part, we use a finite volume well-balanced scheme introduced in [14] to approximate time dependent solutions to Eq. (17). Afterwards, we explore numerically the solutions to system (17) for various sets of parameters. We also compare the Lifshitz-Slyozov diffusive equation with the transport equation (11) and with the transport equation (11) with a constant diffusive term. We will finally explore the case when $\lambda < \lambda_0 = \lim_{L\to 0^+} \Phi(L) => 0$ mentioned previously in the remark of Sec.4.2.

Note that in this section, unlike the previous ones, we are working on a bounded domain $x \in [0, x_{\max}]$ rather than on $\mathbb{R}^+$.

5.1 A well-balanced numerical scheme for system (17)

In the following, we will need to compute some approximations for the stationary solutions $M_{L_{\text{stat}}}$ since we need them in the well-balanced scheme, see later on. Moreover, it will enable us to compare the asymptotic profiles with the stationary solutions in the numerical tests.

Let us recall that stationary solutions $M_{L_{\text{stat}}}$ are defined by an explicit expression given at Eq. (41) with L_{stat} satisfying constraint equation (42). Therefore, to compute this stationary solution, a simple dichotomy method is implemented to find the solution to $\Phi(L) = \lambda$, since the application Φ is increasing in the range of L that interests us, see Figure 3. We use the trapezoidal rule for the computation of the integrals.

Since we are interested in a conservative PDE, we use a finite volume scheme. We also aim at capturing correctly stationary solutions and for that purpose, we implement a well-balanced scheme introduced in [14]. Let us detail the scheme here.

The scheme is based on a change of variables in the PDE (17) to obtain a symmetric operator. This will allow simpler calculations down the line. Denote D_L the spatial operator in the PDE, i.e. :

$$D_L g = \partial_x F(g; x, L) = \partial_x \Big(- v(x, L)g + \partial_x (d(x, L)g) \Big).$$

We recall that the stationary solution associated with the value L is given by :

$$M_L(x) = \frac{C(m, L)}{d(x, L)} \exp\Big(\int_0^x \frac{v(y, L)}{d(y, L)} \mathrm{d}y \Big). \tag{43}$$

This stationary solution satisfies $D_L M_L = 0$ and we can rewrite the operator D_L in the following way :

$$D_L g = \partial_x \Big(d(x, L) M_L \partial_x (\frac{g}{M_L}) \Big).$$

Then we perform the change of variable $h = \frac{g}{\sqrt{M_L}}$ and introduce the new operator $\tilde{D}_L$, which is symmetric for the L^2 inner product :

$$\tilde{D}_L h = \frac{1}{\sqrt{M_L}} D_L (h\sqrt{M_L}) = \frac{1}{\sqrt{M_L}} \partial_x \Big(d(x, L) M_L \partial_x (\frac{h}{\sqrt{M_L}}) \Big).$$

Note that we use an implicit discretization in time in order to avoid a constraining time step for the diffusion operator.

Given a mesh of size $\Delta x > 0$ in space, we discretize the interval $[0, x_{\max}]$ and consider N cells $\mathcal{C}_j = [x_{j-1/2}, x_{j+1/2}]$, $\quad 1 \le j \le N$ centered at point x_j, with $x_j = j\Delta x$ and $x_{j+1/2} = (j + 1/2)\Delta x$. We also introduce a time step $\Delta t > 0$ and the discretization times $t_n = n\Delta t$, $n \in \mathbb{N}$.

We denote by h_j^n an approximation of the average of function h on cell $\mathcal{C}_j$ at time t_n, that is to say $h_j^n \sim \frac{1}{\Delta x}\int_{\mathcal{C}_j} h(t_n,x)\mathrm{d}x$. We also define $M_{L^n,j}$ as an approximation of stationary solution M_{L^n} defined at Eq. (43) at point x_j with $L = L^n$, and $D_{j+1/2}^n$ as an approximation of diffusion coefficient $d(x_{j+1/2}, L^n)$ at point $x_{j+1/2}$ with $L = L^n$, see expression (15).

We denote by $F_{j+1/2}^n$ an approximation of flux $d(x,L)M_L\partial_x(\frac{h}{\sqrt{M_L}})$ at the boundary $x_{j+1/2}$ of cell $\mathcal{C}_j$ at time t_n.

We therefore discretize Eq.(17a) as follows :

$$\begin{aligned}\frac{h_{j+1}^n - h_j^n}{\Delta t} &= \frac{1}{\Delta x\sqrt{M_{L^n,j}}}(F_{j+1/2}^n - F_{j-1/2}^n)\\ &= \frac{1}{\Delta x\sqrt{M_{L^n,j}}}\Big(D_{j+1/2}^n\sqrt{M_{L^n,j+1}M_{L^n,j}}\frac{h_{j+1}^{n+1}/\sqrt{M_{L^n,j+1}} - h_j^{n+1}/\sqrt{M_{L^n,j}}}{\Delta x}\\ &\qquad - D_{j-1/2}^n\sqrt{M_{L^n,j}M_{L^n,j-1}}\frac{h_j^{n+1}/\sqrt{M_{L^n,j}} - h_{j-1}^{n+1}/\sqrt{M_{L^n,j-1}}}{\Delta x}\Big).\end{aligned}$$

Regarding boundary conditions, we want to preserve the zeroth-order moment $\int_0^{x_{\max}} g(t,x)\mathrm{d}x = \int_0^{x_{\max}} g^0(x)\mathrm{d}x$, which implies to use the following null-flux boundary conditions :

$$-v(x,L(t))g(t,x) + \frac{\varepsilon}{2}\partial_x(d(x,L(t))g(t,x))|_{x=0,x_{\max}} = 0.$$

In practice, those boundary conditions are implemented using ghost cells centered at points $-\Delta x$ and $x_{\max}+\Delta x$, and by setting the null-flux conditions $F_{-1/2}^n = F_{N+1/2}^n = 0$.

In order to update the value of L, we derive Eq.(17b) with respect to time and we discretize the equation $\partial_t L = -\int_{\mathbb{R}_+} x\partial_t g(t,x)\mathrm{d}x$, which gives:

$$L^{n+1} = L^n - \Delta x\sum_{i=1}^N x_i(g_i^{n+1} - g_i^n).$$

This update leads to a restriction on the time step Δt to preserve positivity of L^{n+1} as seen in [14].

5.2 Numerical results

The previous numerical scheme enables us to explore the properties of system (17) as a model for adipocyte distribution evolution in time. Table 1 presents the value of most parameters for the simulations. Unless stated otherwise, these parameters shall be fixed for this section. Concerning values of parameters, a few of them are chosen in accordance with biological observations. V_{lipids} and r_0 have fixed given values. The value of γ is taken from [36]. Values of other parameters are chosen as to observe bimodal distributions. We refer the reader to [2] for further investigation into the values of those parameters.

Parameter	Value	Unit	Description	Related equation
α	0.7	nmol h^{-1} μm^{-1}	Lipogenesis surface limited flow rate	Eq.(4)
ρ	200	μm	Lipogenesis saturation in radius cutoff	Eq.(4)
n	3	$\emptyset$	Lipogenesis saturation in radius power	Eq.(4)
κ	0.01	$\emptyset$	Lipogenesis saturation in external lipid constant	Eq.(4)
β	1	nmol h^{-1}	Lipolysis basal flow rate	Eq.(5)
γ	0.27	nmol h^{-1} μm^{-1}	Lipolysis surface limited flow rate	Eq.(5)
χ	0.01	$\emptyset$	Lipolysis saturation in internal lipid constant	Eq.(5)
V_{lipids}	10^6	μm^3	Molar volume of triglycerides	Eq.(1)
r_0	6	μm	Radius of an adipocyte without lipid	Eq.(1)
ε	0.05	$\emptyset$	Diffusion scaling parameter	Eq.(17a)
$x_{\max}$	15	nmol	Maximal lipid size of an adipocyte	Sec. 5.1
N	10^4	$\emptyset$	Number of discretization points	Sec. 5.1

Table 1: Values of parameters for the model

5.2.1 Asymptotic behaviour of the second order Lifshitz-Slyozov system (17)

To begin with, we check that the asymptotic profile obtained with the time evolution of the solution thanks to the previous described scheme coincides with the stationary solution of Sec.4.2.

First, one may assume that given an initial condition (g^0, L^0), the asymptotic behaviour of the system is governed by the two parameters m and λ. This means that given two initial conditions (g_1^0, L_1^0) and (g_2^0, L_2^0) such that $m_1 = m_2$ and $\lambda_1 = \lambda_2$, the stationary solutions are equal. In Figure 4, both initial conditions are Gaussian functions centered at $x_1 = 1$ and $x_2 = 3$ with $m_1 = m_2$ and initial values L_1^0 and L_2^0 are chosen so that $\lambda_1 = \lambda_2$. We indeed observe that the asymptotic profile is the same for these two initial conditions.

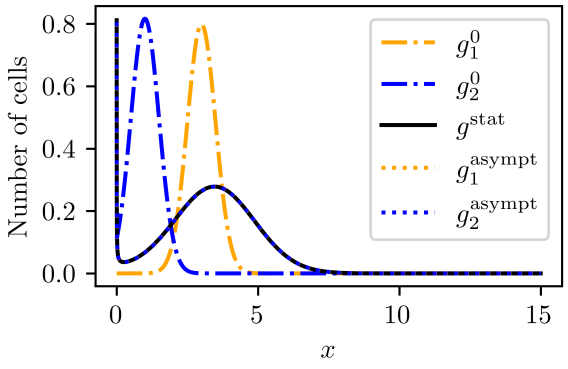

Figure 4: Asymptotic profiles g_1^{asympt} and g_2^{asympt}, from two initial conditions (g_1^0, L_1^0) and (g_2^0, L_2^0) such that $m_1 = m_2$ and $\lambda_1 = \lambda_2$. Parameters of the system are given at Table 1. Note that the stationary solution and the two asymptotic distributions are superimposed.

5.2.2 Bimodality vs unimodality

Since the main aim of the model we develop and study in this paper is to represent bimodality of the distribution on the stationary solution, we check if we effectively find some parameter ranges for which we observe this behaviour. In particular, we investigate the dependency with respect to λ. Note that, since λ is defined by expression (7), we change λ by changing the initial conditions L^0 and g^0, in the case of time evolution of the system, or by changing the value of L^{stat} when considering stationary solutions.

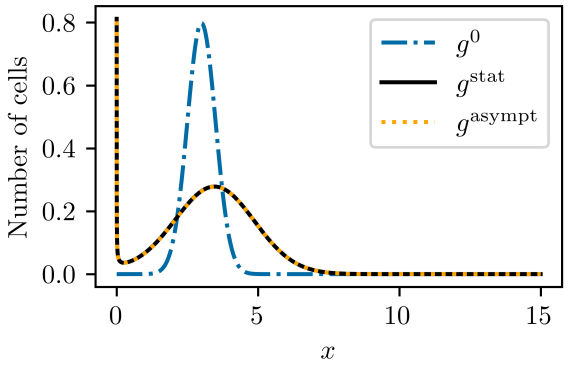

Figure 5: Distributions of adipocytes with respect to size, i.e. amount of lipids, starting with $\lambda = 3.5$ and initial distribution $g^0(x) = C \exp\left(-\frac{1}{2}\left(\frac{x-3}{0.5}\right)^2\right)$ (in dashed blue line) : asymptotic profile (dotted yellow line) and stationary solution (black full line) both present bimodality. Parameters of the system are given at Table 1.

In Figure 5, we plot densities of adipocytes as a function of size x. It shows the result of the scheme starting from a Gaussian initial condition $g^0(x) = C \exp\left(-\frac{1}{2}\left(\frac{x-3}{0.5}\right)^2\right)$ plotted in dashed blue line and L^0 such that $\lambda = 3.5$. The value of C is determined such that $m = 1$. The stationary solution is denoted $g^{\text{stat}} = M_{L_{\text{stat}}}$- in black full line - and the final result of the scheme at time $t = t_{\max}$ is denoted $g(t_{\max}, \cdot)$ and represented in dotted yellow line. $t_{\max}$ is determined such that the relative difference between the size distribution $g(t_{\max}, \cdot)$ and the stationary solution $M_{L_{\text{stat}}}$ is less than 5×10^{-5}. We can observe that bimodality is obtained for the stationary solution as well as for the asymptotic profile of the adipocyte size distribution and that there is a good correspondence between the two functions. Up to some numerical error of order 10^{-12}, both the initial number of cells $m = \int_0^{x_{\max}} g^0(x)\mathrm{d}x$ and the initial amount of lipids λ are conserved, as expected. In Fig.6, we plot the time evolution of the solution : on the left, adipocyte density is displayed as a function of x for various times and on the right, the evolution with respect to time of external lipid concentration L is plotted. We observe that L tends to a stationary value and g to a stationary profile with bimodality as expected.

Now we may investigate the behaviour of the stationary solutions and the asymptotic profiles with respect to λ. A first crucial information is that depending on λ, different types of modality can be observed. Figure 7 presents a case where the stationary solution is unimodal, obtained with

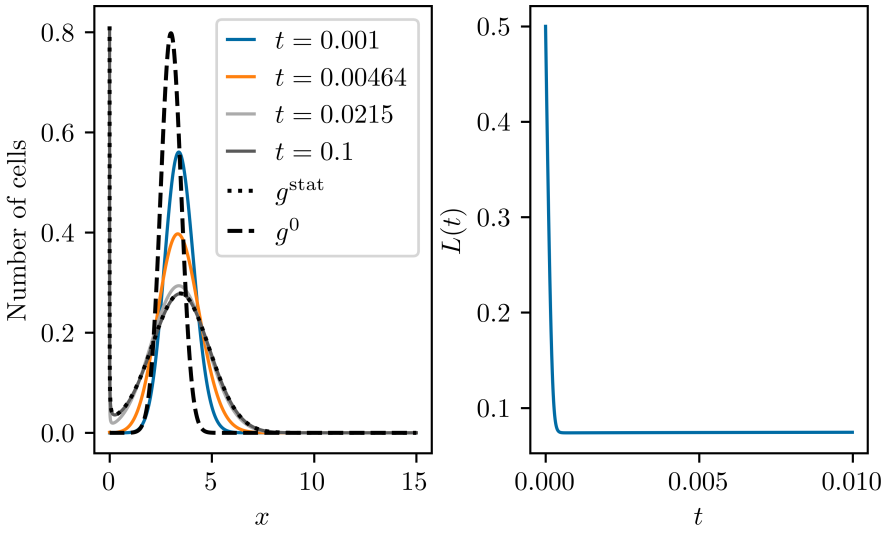

Figure 6: On the left : time evolution of the size distribution with respect to size in the bimodal case; on the right : time evolution of the external lipid concentration. We observe that the asymptotic profile coincides with the computed stationary solution. Parameters of the system are given at Table 1.

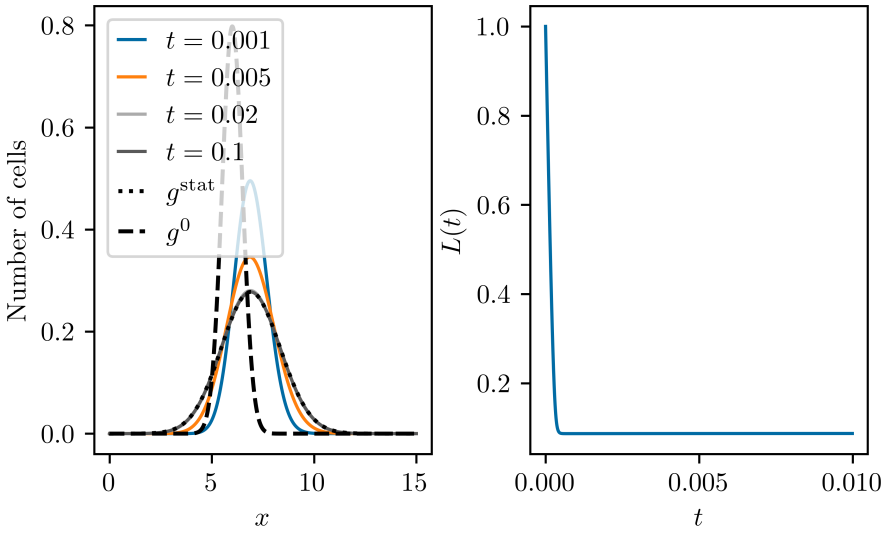

Figure 7: On the left : distributions of adipocytes with respect to size, i.e. amount of lipids, starting with $\lambda = 7$ and initial distribution $g^0(x) = C \exp\left(-\frac{1}{2}\left(\frac{x-6}{0.5}\right)^2\right)$ (in dashed blue line). On the right : time evolution of the external lipid concentration. Asymptotic profile (dotted yellow line) and stationary solution (black full line) both present unimodality. Parameters of the system are given at Table 1.

initial conditions $g^0(x) = C \exp\left(-\frac{1}{2}\left(\frac{x-6}{0.5}\right)^2\right)$, where C is choosen such that $m = 1$, and L^0 such that $\lambda = 7$. We remark that L also tends to a stationary value and densities converge towards a stationary distribution with unimodality. Biologically, we can relate this to the fact that if the amount of lipids in the system is higher, cells have a tendency to put into storage the maximum amount of lipids and thus cells are bigger in average. From a mathematical point of view, since the optima can be linked to the velocity zeros, this means that for bigger λ, two of the zeros of speed V - and therefore two optima - disappear and thus only one zero remains giving rise to a unimodal profile.

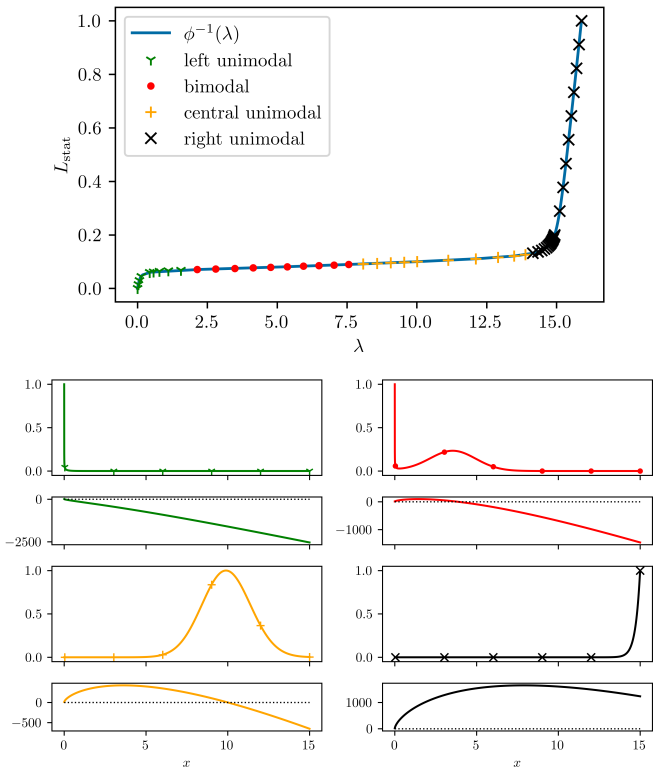

Figure 8: On top : plot of function $\lambda \to \Phi^{-1}(\lambda)$, the inverse function of the one displayed at Fig.3, and type of modality of the stationary solution with respect to the value of λ. On bottom : Normalized stationary solutions for different values of λ, the stationary velocity as a function of x is represented bellow each solution. Top left : left unimodal; top right : bimodal ; bottom left : central unimodal ; bottom right : left unimodal.

More generally, we can investigate the profile modality with respect to the value of λ using the computation of stationary solutions. In Figure 8 on top, we present the type of modality of the stationary solutions as a function of λ. Left (resp. right) unimodality is labeled in green Y (resp. in black x) when a single mode concentrated on the left (resp. right) of the domain is observed. Central unimodal stationary solution is labeled in yellow + when the unique mode is concentrated inside the domain. Bimodality is labeled in red dot.

In Fig.8 on bottom, a plot for each of the 4 types of modality is presented. On the top, we represent the stationary solution $M_{L_{\text{stat}}}$ with respect to x and on the bottom, we plot the stationary velocities with respect to x. Four different values of L_{stat} corresponding to various λ are considered, namely $L_{\text{stat}} = 0.05$ and $\lambda = 0.191$ for the left unimodality (top left, in blue), $L_{\text{stat}} = 0.075$ and $\lambda = 3.52$ for the left bimodality (top right, in green), $L_{\text{stat}} = 0.1$ and $\lambda = 9.96$ for the central unimodality (bottom left, in yellow) and $L_{\text{stat}} = 0.2$ and $\lambda = 14.9$ for the left unimodality (bottom right, in black). For a biological interpretation, left modality is observed when the amount of lipids is too low and thus cells are of relative small sizes. Right modality is a consequence of the amount of lipids being too large and represents the whole cell population approaching its maximal volume. A mathematical interpretation is given by again considering the zeros of the velocity with an influence on the optima of the profile. Left (resp. right) modality is reached when zeros disappear and/or go outside the domain from the left (resp. from the right). The first mode in the bimodal case can also be localized at 0, the smallest zero of the velocity being outside the domain (on the left).

5.2.3 Influence of ε and comparison with a constant diffusion rate D

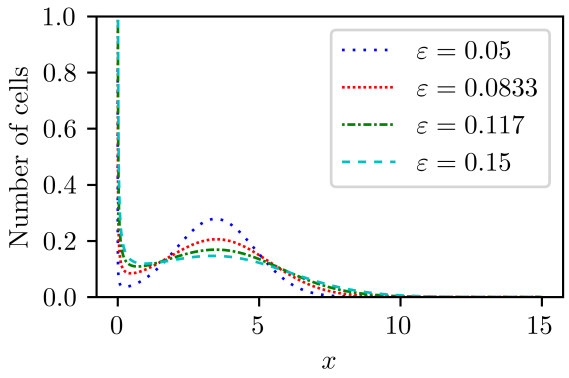

Figure 9: Different stationary solutions depending on the value of ε. We observe that bimodality holds for values of ε small enough. Parameters of the system are given at Table 1.

In this part, we explore the influence of parameter ε on the shape of stationary solutions. We can observe in Figure 9 that higher values of ε smoothen the two maxima of the solution, as expected. For smaller values of ε, the nadir (i.e. the local minimum between the two maxima) gets sharper and for very small ε this may result numerically in taking very small time and space steps. This is easily interpreted as the fact that when $\varepsilon = 0$, we consider the classical Lifshitz-Slyozov system where stationary solutions are sums of Dirac masses which is difficult to obtain numerically without a dedicated scheme.

The choice we made for the diffusion rate is supported by the convergence results from the Becker-Döring to Lifshitz-Syozov model and the behaviour of second order terms. However this choice is not motivated by biological observation. Hence one may make the assumption that the diffusion rate is constant in both time and space. This unfortunately results in quite different results as shown in Figure 10. We point out that to obtain bimodality some parameters need to be readjusted in this case. Hence comparing the solutions of the system under consideration (17) and the solutions with constant diffusion rate proves to be difficult because the behaviour of stationary solutions is heavily dependent on the choice of parameters.

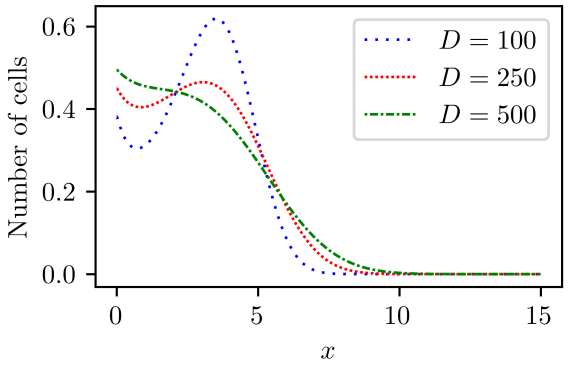

Figure 10: Different stationary solutions depending on the value of diffusion rate D taken as constant in space and time. Parameters of the system are given at Table 1.

We still can make a few comments about the resulting solutions. The constant diffusion rate tends to smoothen the first maximum whereas in the non-constant case, the diffusion is relatively close to zero, leading to a sharper maximum. Our investigation of the available data for adipose cell distribution leads us to believe that non-constant diffusion rates have better chances of making the model fit with the data. We also point out that in the case of constant diffusion, each type of modality, as previously described, is obtainable.

5.2.4 Comparison with the first order model

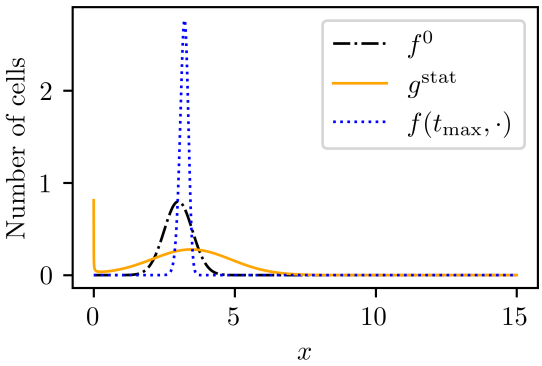

Figure 11: Numerical solution for the first order Lifshitz-Slyozov model (11) (in dotted blue line) compared to the stationary solution of the Lifshitz-Slyozov diffusive model (17) (in orange plain line) with the same parameters and same initial condition (displayed in black dashed -dotted line). The solution to the first order Lifshitz-Slyozov model is expected to converge to a Dirac mass and is displayed for a time before reaching the asymptotic profile.

Stationary solutions for the first order Lifshitz-Slyozov model are not so easily computed theoretically. Nonetheless we can explore these solutions numerically as asymptotic profiles of the solutions

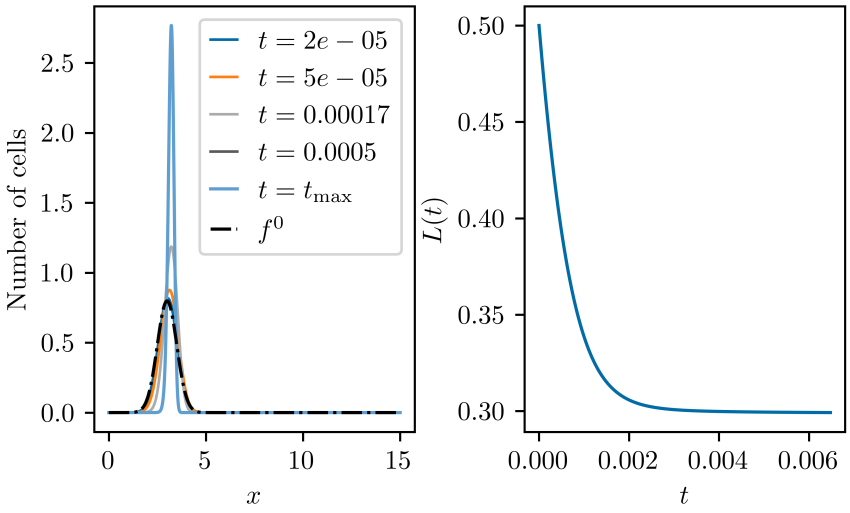

Figure 12: Numerical solution for the first order Lifshitz-Slyozov model (11) with same parameters and initial data as in Fig. 6. On the left : time evolution of the size distribution with respect to size; on the right : time evolution of the external lipid concentration. The solution to the first order Lifshitz-Slyozov model is expected to converge to a Dirac mass and is displayed for a time before reaching the asymptotic profile.

of system (11). For that purpose, we use a standard upwind scheme for transport equations, since the velocity is known. Figure 11 presents the result of an upwind scheme for the Lifshitz-Slyozov model with the same initial conditions and parameters as in Fig. 6. We expect singular stationary state for the first order Lifshitz-Slyozov model. We may interpret stationary state that concentrates at two points as a degenerate bimodal solution. Using the same parameters as in Fig. 6, we can see on Fig. 12 that the solution concentrates to a singular Dirac mass and that in this case we cannot recover bimodality, unlike the case of second-order Lifshitz-Slyozov model, see Fig.11. We also point out that the asymptotic values of L are different in both cases.

By changing initial conditions and the parameter β to $\beta = 100$, we can nonetheless obtain a bimodal solution for the first order Lifshitz-Slyozov model (11) as seen in Fig. 13 on the left. However, by changing the initial condition f^0, we can see on Fig. 13 on the right that we do not obtain the same asymptotic solutions. This leads us to believe that in the case of the first order Lifshitz-Slyozov model the asymptotic solutions depend on the initial condition g^0 and not only on m and λ, unlike for second order Lifshitz-Slyozov model (17).

5.2.5 The case $\lambda < \Phi(0)$

As explained in the remark of Sec.4.2, for different choices of functions a and b than those of the adipocyte model, we may find situations where $\lim_{L\to 0^+} \Phi(L) = \lambda_0 > 0$. In this subsection, we explore the evolution of a solution for a value of λ such that $0 < \lambda < \lambda_0$, that is to say in a case when no smooth stationary solution exists. An example of choice for a and b is $a(x) = 1$ and $b(x) = (x+1)^{2/3}$ and in Fig.14, the function $L \to \Phi(L)$ is displayed in that case.

We show in Figure 15 the time evolution of the density profile (on the left) and of the external

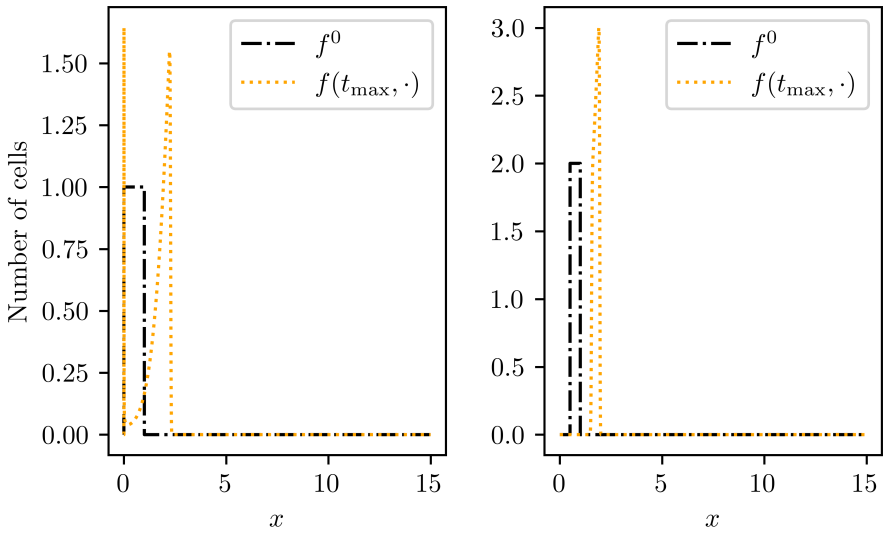

Figure 13: Asymptotic profiles for the first order Lifshitz-Slyozov model (11) with $m = 1$ and $\lambda = 2$. Left : $f^0(x) = C\mathbb{1}_{[\Delta x,1]}(x)$. Right : $f^0(x) = C\mathbb{1}_{[0.5,1]}(x)$. The difference in the initial conditions leads to different profiles. To observe bimodality the parameter β was changed to $\beta = 100$ in both cases.

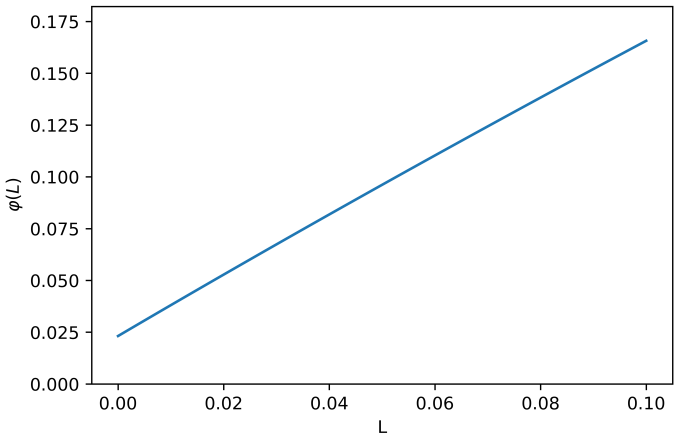

Figure 14: Plot of function $L \to \Phi(L)$ with $a(x) = 1$ and $b(x) = (x+1)^{2/3}$. In that case, $\lim_{L\to 0^+} \Phi(L) \sim 0.025 > 0$ and the existence of smooth stationary solutions for values of λ such that $\lambda < \lambda_0$ is not guaranteed.

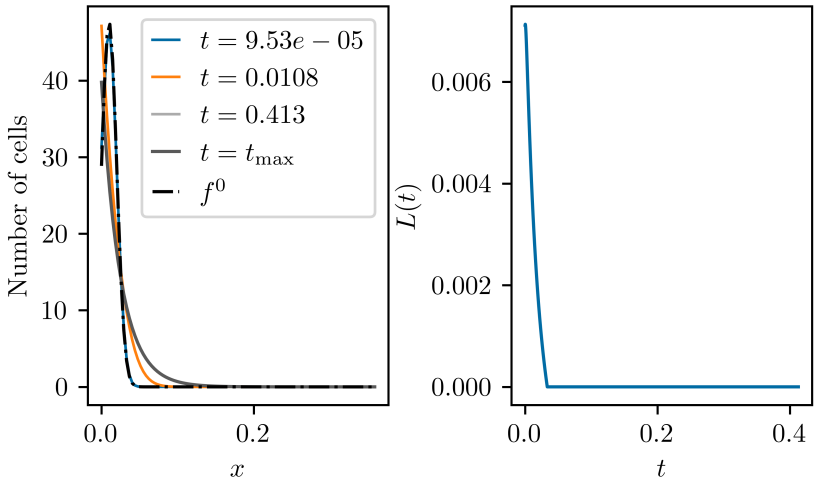

Figure 15: Case when $a(x) = 1$ and $b(x) = (x+1)^{2/3}$ and $\lambda < \lambda_0$. On the left : time evolution of the size distribution with respect to size; on the right : time evolution of the external lipid concentration.

lipid concentration L (on the right) computed numerically in a case where $\lambda < \lambda_0$. We observe that, as expected, L tend to 0 asymptotically and that the adipocyte density seems to converge towards a Dirac mass centered at 0. Numerical simulations prove difficult because of the constraint on Δt to enforce the stability of the numerical scheme. More precisely, this constraint induces that Δt should be bounded above by L^n. Hence as the computation time increases, we observe that the value of L^n tends to zero, as the solution gets closer to the asymptotic profile and therefore that the time step eventually gets smaller than machine precision. In this case, the scheme fails to conserve both λ and m.

6 Conclusion

Our work provides a new approach for looking into convergence from Becker-Döring to Lifshitz-Slyozov, and numerical results indicating that the second order Lifshitz-Slyozov model is better suited to model adipocyte size distribution than previous approach relying on first order Lifshitz-Slyozov model.

The originality of this study lies in the following points :

- a new second order Lifshitz-Slyozov model (17) for adipocyte size distribution with a diffusion term derived from a discrete model,
- Becker-Döring and Lifshitz-Slyozov systems with an unusual velocity (3) -(5) with three zeros and a saturation term in L, which leads to different types of stationary solutions,
- an additional conservation law (8) with respect to classical systems, enforcing uncommon boundary conditions, see Eq. (10) and (16),
- a new proof of convergence result from Becker-Döring solutions to Lifshitz-Slyozov solutions, using tails of distributions, that provides an upper bound on the speed of convergence.

- numerical results showing that bimodal distributions, as well as unimodal profiles, can be obtained asymptotically with system (17), according to the parameters,
- numerical results exploring the influence of parameter ε and comparing the diffusion term of system (17) with a time and space constant coefficient.
- numerical results shows that the second order system (17) provides universal asymptotic profile that does not depend on initial condition (but only on λ, m), contrary to first order system (11).

We believe that the distribution tail approach could be further investigated to show convergence towards the solutions to the second order Lifshitz-Slyozov equation. The asymptotic behaviour of solutions to the second order Lifshitz-Slyozov model will be investigated in future works.

References

[1] P. Arner et al. "Adipose Lipid Turnover and Long-Term Changes in Body Weight". In: *Nature Medicine* 25.9 (2019), pp. 1385–1389.

[2] Chloé Aubdebert et al. "Mathematical modeling of adipose tissue size distributions: parameter identifiability study and estimation with measured adipocyte size distributions in rats".

[3] John M. Ball, Jack Carr, and Oliver Penrose. "The Becker-Döring cluster equations: basic properties and asymptotic behaviour of solutions". In: *Communications in mathematical physics* 104.4 (1986), pp. 657–692.

[4] Richard Becker and Werner Döring. "Kinetische behandlung der keimbildung in übersättigten dämpfen". In: *Annalen der physik* 416.8 (1935), pp. 719–752.

[5] Vincent Calvez et al. "Prion dynamics with size dependency–strain phenomena". In: *Journal of Biological Dynamics* 4.1 (2010), pp. 28–42.

[6] Juan Calvo, Erwan Hingant, and Romain Yvinec. "The Initial-Boundary Value Problem for the Lifshitz–Slyozov Equation with Non-Smooth Rates at the Boundary". In: *Nonlinearity* 34.4 (2021), p. 1975.

[7] José A. Cañizo, Amit Einav, and Bertrand Lods. "Uniform moment propagation for the Becker–Döring equations". en. In: *Proceedings of the Royal Society of Edinburgh: Section A Mathematics* 149.04 (Aug. 2019), pp. 995–1015. DOI: 10.1017/prm.2018.99.

[8] Jean-François Collet and Thierry Goudon. "On solutions of the Lifshitz-Slyozov model". In: *Nonlinearity* 13.4 (2000), p. 1239.

[9] Joseph G. Conlon and André Schlichting. "A Non-Local Problem for the Fokker-Planck Equation Related to the Becker-Döring Model". In: *Discrete and Continuous Dynamical Systems* 39.4 (2019), pp. 1821–1889. DOI: 10.3934/dcds.2019079.

[10] Julien Deschamps, Erwan Hingant, and Romain Yvinec. "Quasi steady state approximation of the small clusters in Becker–Döring equations leads to boundary conditions in the Lifshitz–Slyozov limit". In: *Communications in Mathematical Sciences* 15.5 (2017), pp. 1353–1384. DOI: 10.4310/CMS.2017.v15.n5.a7.

[11] A. Divoux and K. Clement. "Architecture and the Extracellular Matrix: The Still Unappreciated Components of the Adipose Tissue". In: *obesity reviews* 12.5 (2011), e494–e503.

[12] Marie Doumic, Thierry Goudon, and Thomas Lepoutre. "Scaling limit of a discrete prion dynamics model". In: *Communications in Mathematical Sciences* 7.4 (2009), pp. 839–865.

[13] Jérôme Gilleron et al. "Modeling and analysis of adipocytes dynamic with a differentiation process". In: *ESAIM: Proceedings and Surveys* 67 (2020), pp. 210–241.

[14] Thierry Goudon and Laurent Monasse. "Fokker–Planck Approach of Ostwald Ripening: Simulation of a Modified Lifshitz–Slyozov–Wagner System with a Diffusive Correction". In: *SIAM Journal on Scientific Computing* 42.1 (2020), B157–B184.

[15] Meredith L. Greer, Laurent Pujo-Menjouet, and Glenn F. Webb. "A mathematical analysis of the dynamics of prion proliferation". In: *Journal of theoretical biology* 242.3 (2006), pp. 598–606.

[16] S. Hariz and J. F. Collet. "A Modified Version of the Lifshitz-Slyozov Model". In: *Applied mathematics letters* 12.1 (1999), pp. 81–85.

[17] E. Hingant and R. Yvinec. "Deterministic and Stochastic Becker–Döring Equations: Past and Recent Mathematical Developments". en. In: *Stochastic Processes, Multiscale Modeling, and Numerical Methods for Computational Cellular Biology*. Springer, Cham, 2017, pp. 175–204. DOI: 10.1007/978-3-319-62627-7_9.

[18] George A. Jackson and Adrian B. Burd. "Aggregation in the marine environment". In: *Environmental science & technology* 32.19 (1998), pp. 2805–2814.

[19] Junghyo Jo, Zeina Shreif, and Vipul Periwal. "Quantitative Dynamics of Adipose Cells". In: *Adipocyte* 1.2 (2012), pp. 80–88.

[20] Junghyo Jo et al. "Hypertrophy and/or Hyperplasia: Dynamics of Adipose Tissue Growth". In: *PLoS computational biology* 5.3 (2009), e1000324.

[21] Junghyo Jo et al. "Mathematical Models of Adipose Tissue Dynamics". In: *The Mechanobiology of Obesity and Related Diseases*. 2013, pp. 11–34.

[22] Jaeyeon Kim, Gerald M. Saidel, and Satish C. Kalhan. "A Computational Model of Adipose Tissue Metabolism: Evidence for Intracellular Compartmentation and Differential Activation of Lipases". In: *Journal of theoretical biology* 251.3 (2008), pp. 523–540.

[23] Philippe Laurençot. "Weak Solutions to the Lifshitz-Slyozov-Wagner Equation". In: *Indiana University mathematics journal* 50.3 (2001), pp. 1319–1346.

[24] Philippe Laurençot and Stéphane Mischler. "From the becker–döring to the lifshitz–slyozov–wagner equations". In: *Journal of statistical physics* 106.5 (2002), pp. 957–991.

[25] Philippe Laurençot and Christoph Walker. "Well-posedness for a model of prion proliferation dynamics". In: *Journal of Evolution Equations* 7.2 (2007), pp. 241–264.

[26] Kevin Y. Lee et al. "Developmental and Functional Heterogeneity of White Adipocytes within a Single Fat Depot". In: *The EMBO Journal* 38.3 (2019), e99291.

[27] Ilya M. Lifshitz and Vitaly V. Slyozov. "The kinetics of precipitation from supersaturated solid solutions". In: *Journal of physics and chemistry of solids* 19.1 (1961), pp. 35–50.

[28] Barbara Niethammer. "Macroscopic limits of the Becker-Döring equations". In: *Communications in Mathematical Sciences* 2 (Supplemental Issue 2004), pp. 85–92.

[29] Oliver Penrose et al. "Growth of clusters in a first-order phase transition". In: *J. Statist. Phys.* 19.3 (1978), pp. 243–267.

[30] D. Peurichard et al. “Simple mechanical cues could explain adipose tissue morphology”. In: *Journal of Theoretical Biology* 429 (Sept. 21, 2017), pp. 61–81. ISSN: 0022-5193. DOI: 10.1016/j.jtbi.2017.06.030.

[31] Diane Peurichard et al. “Extra-cellular matrix rigidity may dictate the fate of injury outcome”. In: *Journal of theoretical biology* 469 (2019), pp. 127–136.

[32] Vinca Prana et al. “Modeling the Effect of High Calorie Diet on the Interplay between Adipose Tissue, Inflammation, and Diabetes”. In: *Computational and mathematical methods in medicine* 2019 (2019).

[33] Stéphanie Prigent et al. “An efficient kinetic model for assemblies of amyloid fibrils and its application to polyglutamine aggregation”. In: *PloS one* 7.11 (2012), e43273.

[34] André Schlichting. “Macroscopic limit of the Becker–Döring equation via gradient flows”. In: *ESAIM: Control, Optimisation and Calculus of Variations* 25 (2019), p. 22.

[35] Gieri Simonett and Christoph Walker. “On the solvability of a mathematical model for prion proliferation”. In: *Journal of mathematical analysis and applications* 324.1 (2006), pp. 580–603.

[36] H. A. Soula, Alain Geloen, and C. O. Soulage. “Model of adipose tissue cellularity dynamics during food restriction”. In: *Journal of Theoretical Biology* 364 (2015), pp. 189–196.

[37] H. A. Soula et al. “Modelling adipocytes size distribution”. In: *Journal of theoretical biology* 332 (2013), pp. 89–95.

[38] Oleg Varlamov et al. “Single-Cell Analysis of Insulin-Regulated Fatty Acid Uptake in Adipocytes”. In: *American Journal of Physiology-Endocrinology and Metabolism* 299.3 (2010), E486–E496.

[39] Alexis Vasseur et al. “The Beker–Döring System and Its Lifshitz–Slyozov Limit”. In: *SIAM Journal on Applied Mathematics* 62.5 (2002), pp. 1488–1500.

[40] Oliver Wurl et al. “Formation and global distribution of sea-surface microlayers”. In: *Biogeosciences* 8.1 (2011), pp. 121–135.

7 Annex : the rescaling procedure

We start from Becker-Döring system, which may be written as :

$$\begin{cases} \dfrac{dc_i}{dt} = J_{i-1}(c,l) - J_i(c,l),\ \forall i \geq 1, & \text{(44a)} \\ \dfrac{dc_0}{dt} = -J_0(c,l), & \text{(44b)} \\ l(t)\Lambda + \displaystyle\sum_{i=0}^{\infty} i\Lambda c_i(t) = \lambda,\ \forall t \geq 0, & \text{(44c)} \\ l(0) = l^0, \quad c_i(0) = c_i^0,\ \forall i \geq 1. & \text{(44d)} \end{cases}$$

The rescaling procedure we use is akin to the one in [10, 39]. We introduce the following scaling constants :

- $\bar{A}$ rescaling value of $(a_i)_{i\geq 0}$,
- $\bar{B}$ rescaling value of $(b_i)_{i\geq 1}$,
- $\bar{C}$ rescaling value of $(c_i)_{i\geq 0}$,

- $\bar{T}$ rescaling value of the time scale,
- $\bar{\lambda}$ rescaling value of λ.

We previously denoted by Λ the typical size of a vesicle. Hence it plays the role of a rescaling value and should be treated as so.

Recalling hypothesis (H4), we should make an analogous hypothesis on $(a_i)_{i\geq 0}$ and $(b_i)_{i\geq 0}$ so that after rescaling, hypothesis (H4) holds. Hence assume there exists $A, B, \delta > 0$ such that :

$$a_i = Aa(i\delta) \text{ and } b_i = Bb(i\delta), \text{ for all } i \geq 0. \tag{H'4}$$

Now, we introduce the rescaled variables :

$$\begin{aligned}
\bar{a_i} &= \frac{a_i}{\bar{A}}, \ \forall i \geq 0, \\
\bar{b_i} &= \frac{b_i}{\bar{B}}, \ \forall i \geq 1, \\
\bar{t} &= \frac{t}{\bar{T}}, \\
\bar{c_i}(\bar{t}) &= \frac{c_i(\bar{t}\bar{T})}{\bar{C}}, \ \forall i \geq 0, \\
\bar{L}(\bar{t}) &= l(\bar{t}\bar{T})\Lambda.
\end{aligned}$$

The quantity $\bar{L}$ therefore describes the total amount of lipids in the medium instead of the number of lipid vesicles. To have the proper convergence for the functions a and b later on, we relate the rescaling variables $\bar{A}$ and $\bar{B}$ with the constant in hypothesis (H'4) :

$$\bar{A} = A \text{ and } \bar{B} = B.$$

We compute from equation (13) the derivative of $\bar{c_i}$ for $i \geq 1$:

$$\begin{aligned}
\frac{d\bar{c_i}}{dt}(\bar{t}) &= \frac{\bar{T}}{\bar{C}}\frac{dc_i}{dt}(\bar{t}\bar{T}) \\
&= \frac{\bar{T}}{\bar{C}}\Big(a_{i-1}\frac{l(\bar{t}\bar{T})\Lambda}{l(\bar{t}\bar{T})\Lambda + \kappa}c_{i-1}(\bar{t}\bar{T}) - (a_i\frac{l(\bar{t}\bar{T})\Lambda}{l(\bar{t}\bar{T})\Lambda + \kappa} + b_i)c_i(\bar{t}\bar{T}) + b_{i+1}c_{i+1}(\bar{t}\bar{T})\Big) \\
&= \bar{A}\bar{T}\Big(\bar{a}_{i-1}\frac{\bar{L}(\bar{t})}{\bar{L}(\bar{t}) + \kappa}\bar{c}_{i-1}(\bar{t}) - \bar{a}_i\frac{\bar{L}(\bar{t})}{\bar{L}(\bar{t}) + \kappa}\bar{c}_i(\bar{t})\Big) - \bar{B}\bar{T}\Big(\bar{b}_i\bar{c}_i(\bar{t}) - \bar{b}_{i+1}\bar{c}_{i+1}(\bar{t})\Big).
\end{aligned}$$

The derivative of $\bar{c_0}$ writes as :

$$\frac{d\bar{c}_0}{dt}(\bar{t}) = -\bar{A}\bar{T}\bar{a}_0\frac{\bar{L}(\bar{t})}{\bar{L}(\bar{t}) + \kappa}\bar{c}_0(\bar{t}) + \bar{B}\bar{T}\bar{b}_1\bar{c}_1(\bar{t})$$

and the conservation equation for lipids as :

$$\bar{L}(\bar{t}) + \bar{C}\Lambda\sum_{i\geq 1} i\bar{c}_i(\bar{t}) = \lambda.$$

We now relate all the rescaling constants to a single variable $\varepsilon > 0$, such that :

$$\bar{A}\bar{T} = \bar{B}\bar{T} = \frac{1}{\varepsilon}, \ \bar{C}\Lambda = \varepsilon^2 \text{ and } \delta = \varepsilon.$$

At last, we drop the bar above the variables and replace it with ε as superscript to show the dependency of the solution on ε.